JOURNAL OF GEOPHYSICAL RESEARCH, VOL. 114, D12304, doi:10.1029/2008JD011662, 2009



# Methane and nitrous oxide emissions from the ocean: A reassessment using basin-wide observations in the Atlantic

T. S. Rhee,[1] A. J. Kettle,[2,3] and M. O. Andreae[2]

Received 22 December 2008; revised 30 March 2009; accepted 10 April 2009; published 23 June 2009.

[1] We measured the concentrations of nitrous oxide ($N_2O$) and methane ($CH_4$) in the marine boundary layer and surface waters of the Atlantic Ocean from ~50°N to ~50°S during the Atlantic Meridional Transect expedition (AMT-7) in 1998. The cruise track transects a variety of meteorological and oceanographic regimes. Unusually high mixing ratios of atmospheric $CH_4$ were observed in the extratropical Northern Hemisphere, coinciding with globally high levels of $CH_4$ associated with the El Niño event of 1998. Atmospheric $N_2O$ remained nearly invariable during the expedition, with only a small hemispheric difference (0.82 ppb). Throughout the cruise, these gases were saturated or supersaturated in the water. The coastal region was observed to be a significant source of $CH_4$, while upwelling regions acted as strong $N_2O$ emission sources. We estimated the global oceanic emission of $CH_4$ to be 0.6–1.2 Tg $a^{-1}$, comparable to previous estimates from basin-wide observations. However, our estimate turns out to be ~10 times lower than the value in the 1990 to 2007 Intergovernmental Panel on Climate Change (IPCC) reports, which essentially all relied on the estimate by Ehhalt (1974). A bias toward high $CH_4$ saturation anomalies is probably responsible for the overestimation of the marine $CH_4$ source in the IPCC reports. The $CH_4$ saturation anomaly in the ocean appears to have remained constant over an interval of 20 years in spite of the increase of atmospheric $CH_4$, suggesting that the increase of the surface water temperature driven by global warming may be a major factor. Meanwhile, the $N_2O$ emission from the ocean, estimated in the present study to be 0.9–1.7 Tg N $a^{-1}$, is ~3 times lower than the value in the recent IPCC report [*Denman et al.*, 2007], implying either weak upwelling activity or low amounts of dissolved $N_2O$ in upwelling subsurface waters, or both, in the Atlantic.

**Citation:** Rhee, T. S., A. J. Kettle, and M. O. Andreae (2009), Methane and nitrous oxide emissions from the ocean: A reassessment using basin-wide observations in the Atlantic, *J. Geophys. Res.*, *114*, D12304, doi:10.1029/2008JD011662.

## 1. Introduction

[2] Methane ($CH_4$) is an important greenhouse gas, with a radiative forcing strength per molecule and a global warming potential about 20 times as large as carbon dioxide ($CO_2$) on a 100-year horizon [*Ramaswamy et al.*, 2001]. Moreover, it is involved in many ways in atmospheric chemistry, which may result in an indirect positive radiative forcing [*Lelieveld et al.*, 1998].

[3] In view of the significant role of $CH_4$ in global climate and atmospheric chemistry, numerous studies have investigated its atmospheric budget by means of field observations of emission rates in source areas, or of modeling studies [e.g., *Ehhalt et al.*, 2001]. In spite of large progress in constraining and balancing the estimates of source and sink strengths, substantial uncertainties remain, particularly in the estimates of source strengths, owing to their close link to microbial activity. This impedes fully identifying the causes of the interannual variations of the tropospheric $CH_4$ burden. For instance, it has been speculated that the sudden drop in the growth rate of $CH_4$ in 1992 was related to the decrease of surface temperature [*Dutton and Christy*, 1992] and the increase of stratospheric temperature [*Labitzke*, 1994] associated with the eruption of Mount Pinatubo. The surface cooling may have lead to a reduction of wetland emissions [*Hogan and Harriss*, 1994; *Walter et al.*, 2001], while the stratospheric warming produced an increase in the concentration of the OH radical due to enhanced $O_3$ destruction in the stratosphere, which allows more UV light to reach the troposphere [*Bekki et al.*, 1994]. In addition, reduced biomass burning activity [*Lowe et al.*, 1997] and the decrease of fossil fuel emissions from the former Soviet Union [*Dlugokencky et al.*, 1994] have been suggested as causes, but no direct evidence was given. By the same token, the cause of the positive anomaly of global $CH_4$ growth rate in 1998 has not been identified, although

[1]Center of Polar Climate Sciences, Korea Polar Research Institute, Incheon, Korea.
[2]Biogeochemistry Department, Max Planck Institute for Chemistry, Mainz, Germany.
[3]Now at Department of Earth Sciences, State University of New York at Oswego, Oswego, New York, USA.


0148-0227/09/2008JD011662$09.00

large emissions from wetlands and the direct and indirect impacts of active biomass burning in Indonesian and boreal forests have been suggested as major factors [*Butler et al.*, 2005; *Chen and Prinn*, 2006; *Dlugokencky et al.*, 2001; *Langenfelds et al.*, 2002; *Mikaloff Fletcher et al.*, 2004; *van der Werf et al.*, 2004].

[4] Nitrous oxide ($N_2O$) has a ~300 times greater radiative forcing potential per mass (or molecule) than $CO_2$ on a 100-year horizon [*Ramaswamy et al.*, 2001]. Its long lifetime (~120 years) in the troposphere enables $N_2O$ molecules to reach the stratosphere, where they decompose partly (~6%) to nitric oxide (NO) by reacting with $O(^1D)$. Thus, $N_2O$ is the principal source of $NO_x$ in the stratosphere, where it promotes ozone depletion [*Crutzen*, 1996]. In spite of the significant role of $N_2O$ in climate and the stratospheric ozone budget, its emission strengths have not been well quantified, owing mostly to the difficulties in the estimation of the heterogeneous emissions from soils. The oceanic source strength for $N_2O$ has been rather well constrained because of its homogeneous emission, except in upwelling and coastal areas where hot spots are dominant [*Bange et al.*, 1996a].

[5] The ocean has been identified as a considerable global source of natural $N_2O$ and a minor contributor of $CH_4$. For instance, *Nevison et al.* [1995] estimated the global $N_2O$ flux from the ocean as 4 (1.2–6.8) Tg N $a^{-1}$ (conventionally expressed in mass units of nitrogen) on the basis of observations worldwide. This corresponds to ~40% of all natural sources [*Denman et al.*, 2007]. The first estimates of the oceanic $CH_4$ source were as high as 10–20 Tg $a^{-1}$ [*Bange et al.*, 1994; *Ehhalt*, 1974; *Lambert and Schmidt*, 1993], and these values have been used in the successive Intergovernmental Panel for Climate Change (IPCC) reports. A later study, based on observations in the Pacific during the SAGA and RITS scientific expeditions, has yielded a much lower estimate for $CH_4$ of 0.4 (0.2–0.6) Tg $a^{-1}$ [*Bates et al.*, 1996]. Using this estimate, the ocean only contributes ~0.07% to total $CH_4$ emissions. Given that the Pacific occupies 50% of the world ocean, the extrapolation of the flux from the Pacific to the world ocean cannot account for the large discrepancy between estimates. Since $CH_4$ plays an important role in climate change and in atmospheric chemistry, it is essential to resolve these large discrepancies and to evaluate reliably the budgets of these gases in the atmosphere. In this study, we investigated the fluxes of $N_2O$ and $CH_4$ from the ocean using basin-wide observations in the Atlantic, and compared them with previous evaluations.

[6] Our investigations were carried out aboard the RRS *James Clark Ross* during the seventh expedition of the Atlantic Meridional Transect program (AMT-7). One of the main objectives in the AMT program is to investigate the response of ecosystems in the Atlantic to change in global climate due to the anthropogenic emission of radiative forcing gases; see *Aiken et al.* [2000] and *Robinson et al.* [2006] for details of the AMT program. On AMT-7, the program determined physical and biological oceanographic conditions along the cruise track by the routine measurement of sea surface temperature and salinity, plankton distribution and optical properties of seawater, and by profile observations at hydrographic stations. Additionally, radiosondes were launched on a regular basis along the cruise track for monitoring surface atmospheric temperature, pressure, and relative humidity. This assisted us in evaluating the variation of atmospheric mixing ratios of trace gases encountered during the expedition. The campaign commenced on 12 September and ended on 25 October 1998. The cruise track went from ~50°N, Grimsby, UK, to ~50°S, Stanley, Falkland Islands, UK. (Figure 1). During this period, over 2200 measurements of $N_2O$ and $CH_4$ in the surface water and overlying air were made.

## 2. Meteorological and Oceanographic Situations During the AMT-7

[7] The meteorological conditions along the cruise track are described on the basis of HYSPLIT model calculations of 4-day back trajectories of air masses (Figure 1), complemented by in situ observations of surface atmospheric temperature (SAT) and pressure, wind speed and direction (Figure 2), and vertical profiles of relative humidity (RH) acquired from radiosondes launched on board (Figure 3). The various air masses characterized by these meteorological parameters are listed in Table 1 and are described in detail in the auxiliary material.[1]

[8] A comprehensive oceanographic overview along the tracks of a series of the Atlantic Meridional Transect (AMT) cruises has been described in detail by *Aiken et al.* [2000], and the specific details of the AMT-7 campaign by *Kettle et al.* [2001]. The oceanographic situation is illustrated in Figure 4 for the in situ observations of sea surface temperature (SST), sea surface salinity (SSS), fluorescence, and chlorophyll *a* (chl *a*) concentration to aid in the interpretation of dissolved gas distributions observed along the track. In addition, climatological data for SST and SSS in the Compressed Marine Reports–Product 5 of the Comprehensive Ocean-Atmosphere Data Set (COADS/CMR-5) [*Woodruff et al.*, 1987] are superimposed for comparison and to extrapolate the gas flux estimates to the global scale, which is one of main objectives of this paper. These are mean values of 45 years of climatological data, covering 1945 through 1989, and were binned as 1° × 1° monthly means.

[9] On the basis of the physical and biological properties of surface seawater along the cruise track (see auxiliary material), we divide the study area into three typical oceanographic regions: open ocean, coastal region, and coastal upwelling zone, as indicated in Figure 4. The equatorial upwelling zone is categorized as open ocean. The chl *a* concentration is particularly useful for classifying the cruise track (see Figure 4), considering that dissolved concentrations of $CH_4$ and $N_2O$ are closely linked to biological activity [e.g., *Elkins et al.*, 1978; *Karl and Tilbrook*, 1994].

## 3. Experiments

[10] Two sets of measurements were carried out on board; (1) $CH_4$ and $N_2O$ in surface air and the corresponding dissolved gases in the waters of the upper mixed layer were monitored along the cruise track and (2) depth profiles of

[1] Auxiliary materials are available in the HTML. doi:10.1029/2008JD011662.

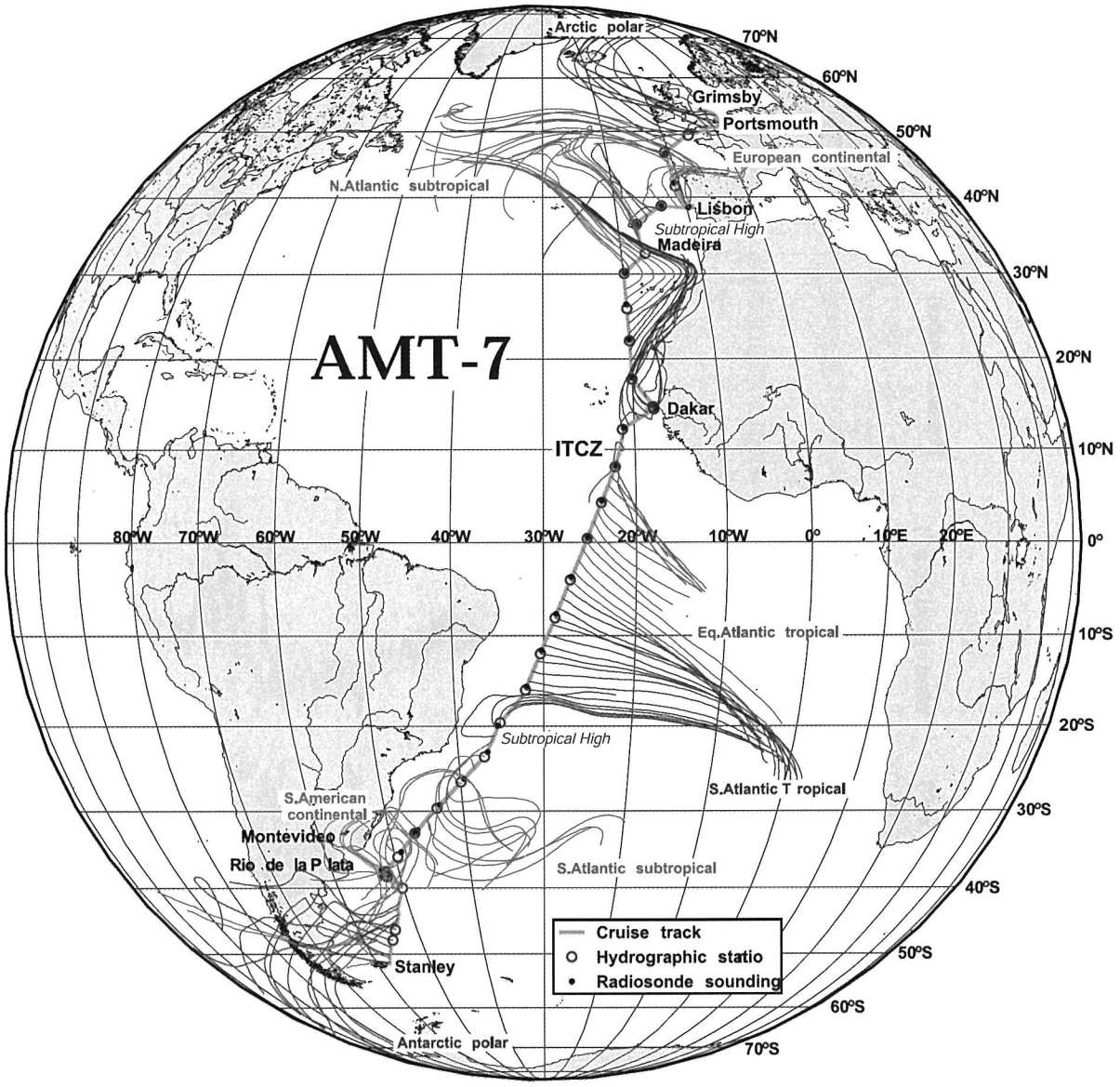


**Figure 1.** Cruise track of the Seventh Atlantic Meridional Transect (AMT-7) and 4-day backward trajectories along the track. Air masses encountered during the cruise are indicated.

$N_2O$ in the euphotic zone (~200 m) were made at the hydrographic stations (Figure 1).

### 3.1. Sampling Methods

#### 3.1.1. Underway Sampling

[11] The air sampling inlet was mounted on the foremast of the ship below the meteorological platform, 19 m above the sea surface and ~53 m from the exhaust of the ship, to avoid flow of contaminated air into the detector. Air samples were drawn through polyethylene inner-coated aluminum tubing (Dekabon) at a flow rate of ~10 L $min^{-1}$ using a small pump (Air Cadet). The total length of the tubing was ~90 m and the residence time of the air in the tubing was approximately 15 s. The inlet was fitted with a funnel that was directed downward to prevent rainwater or sea spray from entering the tubing and the analyzer.

[12] The RRS *James Clark Ross* provides an uncontaminated surface seawater supply system, whose inlet is mounted below the keel of the ship at a depth of ~6 m; seawater was drawn by either of two pumps into the main plumbing at 120 or 230 L $min^{-1}$ through a stainless steel filter with a mesh size of 5 mm. The filter was cleaned every day. Part of the filtered water was pumped into a Weiss-type equilibrator [*Butler et al.*, 1988; *Weiss et al.*, 1992] and continuously showered at a rate of 24 to 30 L $min^{-1}$ through the headspace of the equilibrator. The equilibrator had a headspace of 21 L, and was mounted at the outside of the laboratory. An air sample of 200 mL was withdrawn from the headspace every hour to flush two sample loops for analyses of $CH_4$ and $N_2O$. Since the *e*-folding times for equilibration of $CH_4$ and $N_2O$ are ~20 min and ~1 min,

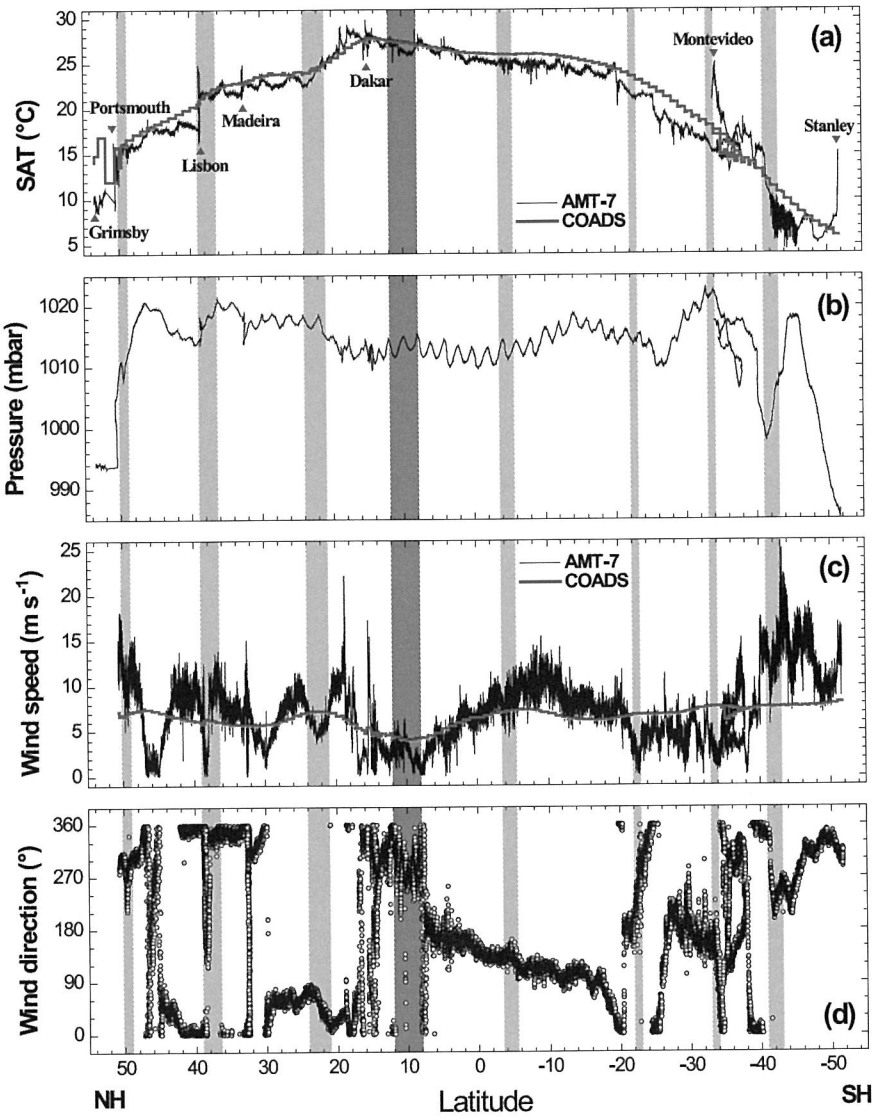


**Figure 2.** Meteorological parameters obtained along the cruise track. Light gray bars indicate meteorological episodes encountered during the campaign (see Table 1). The dark gray bar represents the Intertropical Convergence Zone (ITCZ). Locations of the ports called are shown in Figure 2a. Climatological surface air temperature (SAT) and wind speed from COADS/CMR-5 are shown by a red line in Figures 2a and 2c.

respectively, a sampling interval of 1 h is enough to reach equilibrium of dissolved $CH_4$ and $N_2O$ [*Johnson*, 1999].

### 3.1.2. Discrete Sampling of Dissolved $N_2O$

[13] Seawater from different water depths was collected in 30-L Niskin bottles attached to a Rosette water sampling system with a conductivity-temperature-depth (CTD) sensor. Subsamples of seawater were drawn into a specially designed glass jar for the analysis of dissolved gases. The water sampling method using the glass jar is described in detail by *Bange et al.* [2001] and *Rhee* [2000]. In brief, once the container was sufficiently rinsed, the seawater sample was filled into the glass jar taking care not to trap bubbles inside. A precisely known volume of helium (99.9999%, Linde) was then injected into the glass jar using a calibrated gas-tight syringe (SGE™) to displace an identical volume of water, while the pressure of the headspace inside was maintained at ambient pressure. Around 0.1 mL of saturated $HgCl_2$ was then injected into the glass jar to avoid biological production of $N_2O$ during equilibration. The headspace air in the glass jar was sampled within 12 h using a gas-tight syringe. In order for the headspace to remain at ambient pressure while taking the headspace air, one of the stopcocks in the glass jar was connected by a Tygon tube to a burette filled with water, and then the stopcock was opened. Water in the burette was drawn into the glass jar to maintain the ambient pressure while the headspace air was sampled. During this procedure, considerable care was taken to make certain that no ambient air was entrained into the glass container.

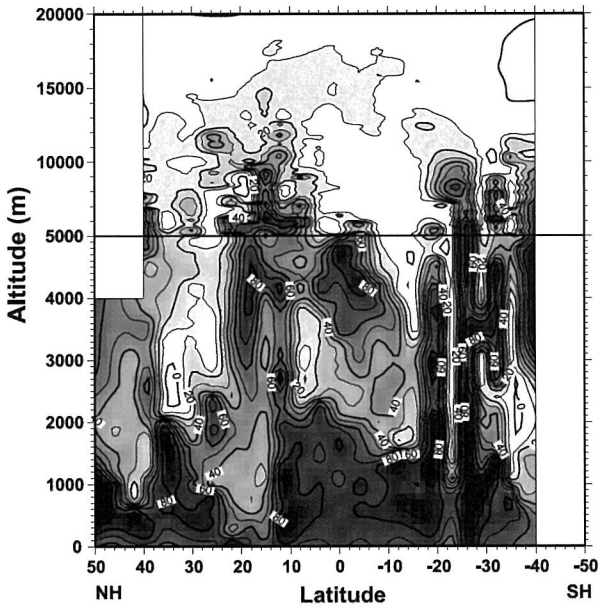


**Figure 3.** Relative humidity (%) obtained from radiosonde soundings along the cruise track. The sounding locations are shown in Figure 1.

### 3.2. Determination of Mixing Ratios

[14] $N_2O$ and $CH_4$ were analyzed by an automated Hewlett-Packard gas chromatographic system (HP 5890). Samples of ambient air, or headspace air from the equilibrator were delivered to the analyzer using a small pump (Air Cadet). The headspace air sample from a glass jar was injected manually to an injection port in the gas chromatographic system. The air sample was dehumidified by passing it through Sicapent™ ($P_2O_5$ desiccant with indicator, Merck) before it entered the sample loops that were enclosed in the same oven as the gas chromatographic columns to keep the temperature of the sample loops constant. Loading and injection of air samples in the sample loops were performed by switching a 2-position 10-port Valco valve (VICI). The separation of $N_2O$ and $CH_4$ was achieved using the same packed columns ($1/8'' \times 3$ ft) filled with carbon molecular sieve, Spherocarb™ (mesh 100/120, Phase Separations, Inc.), at a constant oven temperature of 90°C, with the carrier gases Ar/$CH_4$ (5%) (ECD grade, Linde) and He (99.9999%, Linde) flowing at 50 mL $min^{-1}$ and 40 mL $min^{-1}$, respectively. $N_2O$ and $CH_4$ were detected by an electron capture detector (ECD) at 350°C and a flame ionization detector (FID) at 250°C, respectively. For the FID, $H_2$ and synthetic air were supplied at ~30 mL $min^{-1}$ and ~250 mL $min^{-1}$, respectively.

[15] The gas chromatographic system was calibrated with two standard gases such that samples from the ambient air, equilibrator headspace, and two standard gases were measured alternately to minimize the random error due to the drift of the detector. The $N_2O$ mixing ratios of the two standard gases were calibrated against the SIO-1993 standard scale, and the $CH_4$ mixing ratios were calibrated against the NOAA standard scale. One more high concentration of standard gas (618(±2%) ppb $N_2O$) was purchased from a commercial company to calibrate the high concentrations of dissolved $N_2O$ that were often observed in deep water samples.

### 3.3. Auxiliary Parameters

[16] The RRS *James Clark Ross* was equipped with an underway monitoring system for hydrography (SST, SSS), meteorology (SAT, pressure, wind speed, wind direction), and optical parameters (fluorescence and absorption of surface seawater, thermal infrared radiation (TIR), and photosynthetically available radiation (PAR)). In addition, vertical profiles of temperature, salinity, and optical parameters (fluorescence absorption, PAR, and attenuation) were obtained at the hydrographic stations; see *Kettle et al.* [2001] for detailed information. For correcting the temperature effect on solubility, the water temperature in the equilibrator was monitored.

## 4. Data Treatment and Reduction

[17] The equilibrator was designed such that the pressure inside is the same as that outside. Change in seawater temperatures occurring during the flow to the equilibrator ranged from −0.6°C to 1.5°C, which directly affects the solubility of dissolved gases in the equilibrator. For instance, warming results in the increase of partial pressure inside the equilibrator which in turn leads to high apparent dissolved

**Table 1.** $CH_4$ and $N_2O$ Mixing Ratios for the Various Air Masses Encountered in the Marine Boundary Layer Along the Cruise Track[a]

| | | $CH_4$ (ppb) | | | $N_2O$ (ppb) | | |
|---|---|---|---|---|---|---|---|
| Air Masses | Latitude | Mean | SE | n | Mean | SE | n |
| Arctic Polar | 53°N–50.2°N | 1867 | 4 | 12 | 315.8 | 0.3 | 12 |
| Polar front | 50.2°N–49°N | 1817 | 3 | 34 | 314.3 | 0.1 | 34 |
| North Atlantic subtropical | 49°N–39°N | 1816 | 1 | 120 | 314.7 | 0.1 | 119 |
| Subtropical front | 39°N–36.5°N | 1807 | 2 | 92 | 315.1 | 0.1 | 87 |
| North Atlantic subtropical | 36.5°N–24°N | 1815 | 1 | 214 | 314.9 | 0.1 | 215 |
| Subtropical high | 24°N–21°N | 1773 | 2 | 27 | 315.2 | 0.2 | 27 |
| Northwest African tropical | 21°N–12°N | 1773 | 1 | 154 | 315.0 | 0.1 | 157 |
| ITCZ | 12°N–8°N | 1740 | 2 | 33 | 314.6 | 0.2 | 33 |
| Equatorial Atlantic tropical | 8°N–3.5°S | 1724 | 1 | 119 | 314.4 | 0.1 | 120 |
| Subtropical high | 3.5°S–5.5°S | 1712 | 3 | 22 | 313.8 | 0.3 | 22 |
| South Atlantic tropical | 5.5°S–22°S | 1717 | 1 | 173 | 313.9 | 0.1 | 180 |
| Subtropical high | 22°S–23°S | 1714 | 3 | 11 | 313.8 | 0.3 | 11 |
| South Atlantic subtropical | 23°S–33°S | 1716 | 1 | 143 | 313.9 | 0.1 | 144 |
| Subtropical front | 33°S–34°S | 1711 | 7 | 13 | 313.0 | 0.4 | 15 |
| South American continent | 34°S–41°S | 1748 | 3 | 194 | 314.2 | 0.1 | 192 |
| Polar front | 41°S–43°S | 1731 | 6 | 23 | 314.1 | 0.2 | 23 |
| Antarctic polar | 43°S–53°S | 1711 | 2 | 103 | 314.4 | 0.1 | 103 |
| | Northern Hemisphere | 1800 | 13 | 663 | 314.9 | 0.2 | 661 |
| | Southern Hemisphere | 1721 | 4 | 824 | 314.1 | 0.2 | 833 |
| | Global | 1752 | 12 | 1487 | 314.4 | 0.2 | 1494 |

[a]Abbreviations: SE, standard error (sd/$\sqrt{n}$); n, the number of measurements. The last three rows indicate the hemispheric and global mean values of $CH_4$ and $N_2O$.

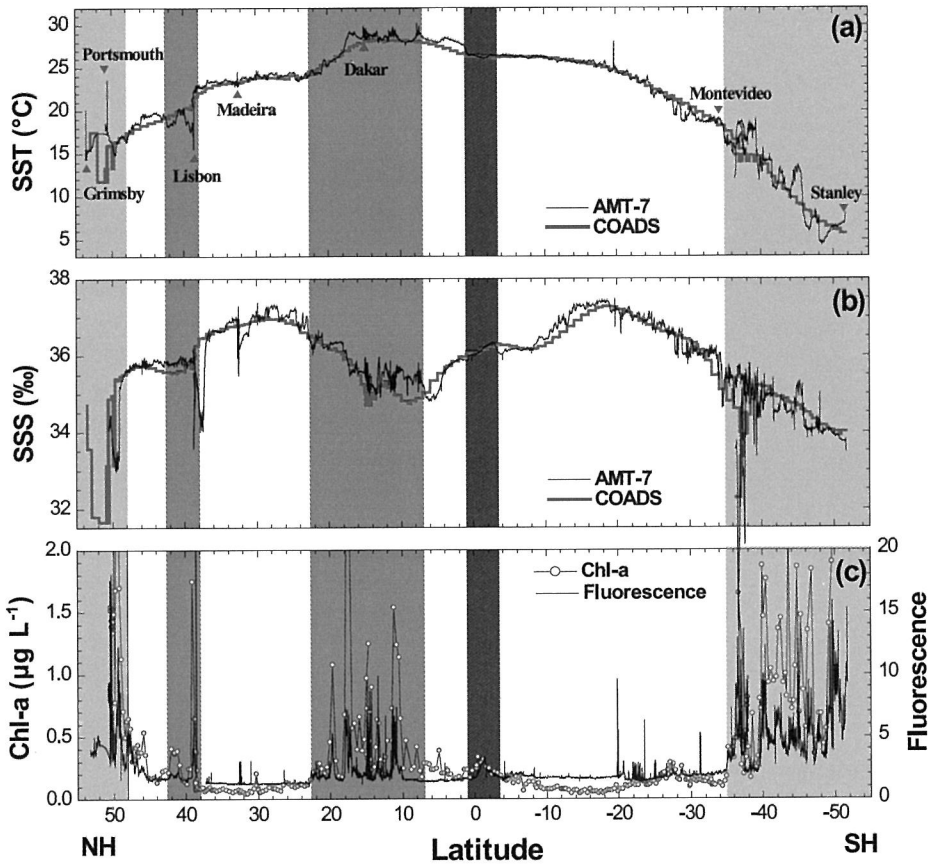


**Figure 4.** (a) Sea surface temperature (SST), (b) sea surface salinity (SSS), and (c) chlorophyll *a* and fluorescence along the cruise track. Unit of fluorescence is arbitrary. Light gray indicates the coastal region, gray is the coastal upwelling zone, and dark gray is the equatorial upwelling zone. The remainder of the transect is assigned as open ocean.

gas concentrations. Corrections for temperature changes have been made on the basis of the conservation of the dissolved concentration in the water, as given by *Butler et al.* [1988]:

$$f_w = f_e \times \frac{K_{oe}}{K_{ow}} \tag{1}$$

for $N_2O$ or

$$p_w = p_e \frac{\beta_e \rho_w}{\beta_w \rho_e} \tag{2}$$

for $CH_4$, where $f$ and $p$ denote fugacity and partial pressure, respectively, $K_0$ is the reciprocal of Henry's law constant in units of mol $kg^{-1}$ $atm^{-1}$, $\beta$ is the Bunsen coefficient, and $\rho$ indicates the density of seawater. The subscripts, $w$ and $e$, denote seawater in situ, and in the equilibrator, respectively. The solubility of $N_2O$ and $CH_4$ were calculated using empirical equations from *Weiss and Price* [1980] and *Wiesenburg and Guinasso* [1979], respectively, and the density of seawater by *Millero and Poisson* [1981].

[18] Dissolved gas concentrations, $C_w$, in the discrete samples were calculated by using the equation

$$C_w = \frac{x_i(P - p\mathrm{H_2O})}{\rho_{sw} RT}\left(L_i + \frac{V_a}{V_w}\right), \tag{3}$$

where $x_i$ indicates the dry mixing ratio of gas $i$, $P$ is the ambient pressure, $p\mathrm{H_2O}$ is the water vapor pressure, $\rho_{sw}$ is the density of seawater when the dissolved gas was sampled, $R$ is the gas constant, $T$ is the absolute temperature of the glass container, $L_i$ is the Ostwald solubility of gas $i$, and $V_a$ and $V_w$ are the volumes of the headspace and the water in the glass container, respectively.

[19] Abnormally high concentrations were often encountered for the underway measurements when the ship was stopped on station or near port. In particular, the influence of exhaust from the ship was clearly observed by the dramatic increase in the carbon monoxide (CO) mixing ratio in the air [*Rhee*, 2000]. Also observed was erratic change in dissolved $CH_4$ when the ship was anchored near Madeira Island, probably due to the influence of wastes from the ship. These data were eliminated.

## 5. Results

### 5.1. Atmospheric Variations Over the Atlantic

#### 5.1.1. Methane

[20] The background $CH_4$ mixing ratios observed in the marine boundary layer (MBL) throughout the cruise varied from ~1870 ppb in the high Northern Hemisphere to ~1710 ppb in the high Southern Hemisphere with a distinct

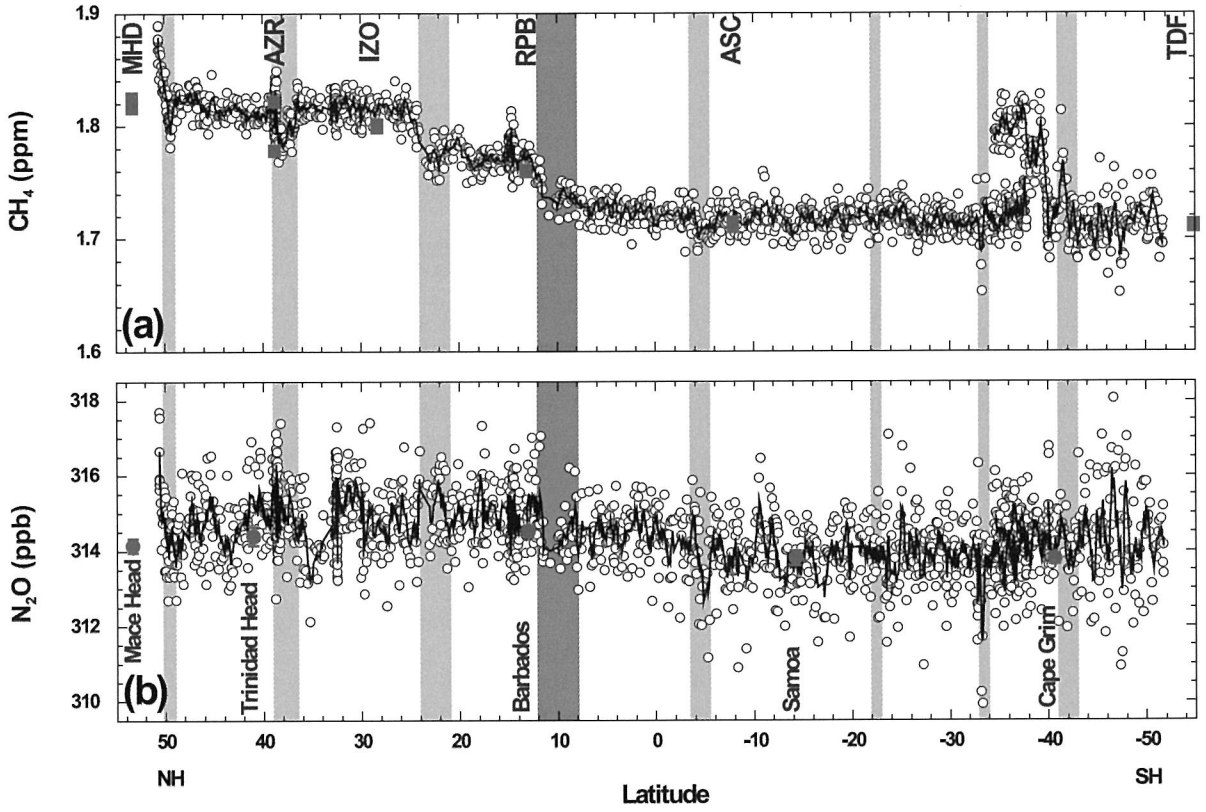


**Figure 5.** Mixing ratios of (a) $CH_4$ and (b) $N_2O$ in the marine boundary layer along the cruise track. Circles are individual measurements, and solid lines indicate five-point running averages. Gray bars represent meteorological events as shown in Figure 2. Red rectangles in Figure 5a indicate the $CH_4$ mixing ratios at the NOAA/ESRL stations noted on the top of the plot, and the red solid circles in Figure 5b represent the mean values of $N_2O$ mixing ratios at the AGAGE stations noted on the bottom of the plot, for the period similar to the AMT-7 cruise.

north-to-south gradient (see Figure 5a). North of the Intertropical Convergence Zone (ITCZ), $CH_4$ mixing ratios varied with the source of air masses as delineated in Table 1, except for the point sources near ports (e.g., Portsmouth, Lisbon, and Dakar). In the south, however, $CH_4$ shows little dependence on regional air masses, except for the air mass coming from the South American continent, indicating a fairly homogeneous distribution over the South Atlantic.

[21] Data from NOAA/ESRL network stations, for air samples collected within a time window of ~3 days with respect to the in situ measurement on board, confirmed our "background" observations in the open ocean (Figure 5a). In particular, the abnormally low $CH_4$ mixing ratio observed at the Azores station (AZR) matches our observations, supporting the synoptic scales of $CH_4$ variation captured during the cruise. The values observed at the Izaña station (IZO) located at 2360 m above sea level (asl) are ~15 ppb lower than the mean value in the MBL between 36.5°N and 24°N (1815 ppb), suggesting a vertical gradient of decreasing $CH_4$ mixing ratios with altitude in the Northern Hemisphere [*Matsueda et al.*, 1993].

[22] As marked by gray bars in Figure 5a, the meteorological episodes encountered during the cruise produced $CH_4$ anomalies; the decrease of $CH_4$ mixing ratios observed in the vicinity of 38°N and 22°N coincided with a subtropical front and a subtropical high, and the dip near 50°N is collocated with a polar front. Since such low $CH_4$ mixing ratios were not observed elsewhere in the MBL north of 24°N, they may be indicative of subsiding air masses from the free troposphere.

[23] Another interesting feature observed north of the ITCZ is the sharp change of the $CH_4$ mixing ratio at ~22°N. The higher background mixing ratios observed north of ~22°N are probably due to the increase in $CH_4$ emissions from boreal wetlands and biomass burning, the $CH_4$ sources that unexpectedly enhanced the global $CH_4$ burden in 1998 [*Dlugokencky et al.*, 2001; *Langenfelds et al.*, 2002; *van der Werf et al.*, 2004]. As mentioned earlier, the year 1998 experienced unusually high surface temperatures and active wildfires, both of which were associated with a strong El Niño–Southern Oscillation (ENSO) cycle [*Bell et al.*, 1999; *van der Werf et al.*, 2004]. The former results in the enhancement of $CH_4$ emissions from wetlands, the largest natural source. *Dlugokencky et al.* [2001] estimated the effect of the increase of temperature and precipitation on $CH_4$ emissions from wetlands, and found the estimate to be consistent with the observed $CH_4$ emission anomaly in 1998, suggesting the $CH_4$ emission from wet-

lands to be a major contributor. It has been suggested that active biomass burning in Russia and Canada in 1998 contributed to the anomaly of $CH_4$ at 2.9–4.7 Tg $a^{-1}$ [*Kasischke and Bruhwiler*, 2002], which corresponds to 23–37% of the $CH_4$ emission anomaly in the high Northern Hemisphere relative to the growth rate in 1999. *Morimoto et al.* [2006] estimated 1/3 of the growth of $CH_4$ in 1998 to be from biomass burning, and the remainder to be from wetlands, consistent with the estimation by *Kasischke and Bruhwiler* [2002].

[24] Southward of 22°N down to the ITCZ, the $CH_4$ mixing ratios dropped by ~42 ppb and then remained almost constant (Table 1). The prevailing easterly wind from northwest Africa (Figure 1), the dry ambient air (Figure 3), as well as the conspicuously low $CH_4$ mixing ratios together delineate the zonal isolation by the Hadley cell in this segment of the cruise. The small rise (~10 ppb) in $CH_4$ observed from 18°N to 21°N coincides with high winds (~10 m $s^{-1}$) and a rise in SAT (Figure 2), indicating that the wind blew from the Sahara desert carrying an air mass that could have mixed with high Northern Hemispheric air, as we also observed enhanced CO mixing ratios (by ~20 ppb) during the same episode [*Rhee*, 2000].

[25] As the ship passed the ITCZ, $CH_4$ mixing ratios dropped step-like with a sharp boundary. A similar sudden drop of $CH_4$ at the ITCZ has also been observed in the Pacific, where a difference of ~50 ppb across the ITCZ [*Matsueda et al.*, 1993] was recorded. South of the ITCZ, $CH_4$ continued to decrease slowly southward, but with a very gentle slope south of 5°S. There was little variability, except for the polluted source area near the Rio de la Plata. The $CH_4$ mixing ratios near Montevideo (~110 ppb larger than the ~1716 ppb background value) represented the largest pollution event encountered during the cruise. When the air mass switched and blew from Antarctica, the background values typical of the Southern Hemisphere returned. Approaching the Falkland Islands, the $CH_4$ mixing ratios increased a little, probably owing to local pollution.

#### 5.1.2. Nitrous Oxide

[26] In contrast to $CH_4$, there were no distinctive changes in the $N_2O$ mixing ratios due to episodic events or different air masses. $N_2O$ remained around ~314(±1) ppb throughout the cruise (Table 1 and Figure 5b). Zonally area-weighted mean values for the two hemispheres show an interhemispheric difference of 0.82 (±0.27, 1 standard error) ppb, which is not significantly different from the value of 0.97 ppb observed in the west Pacific in the El Niño year of 1987 [*Butler et al.*, 1989], and which is virtually the same as the difference of 0.8 ppb observed at remote stations from 1976 to 1980 [*Weiss*, 1981]. Fifteen years of long-term observations in the northern and western Pacific confirmed the same interhemispheric difference of ~0.8 ppb [*Ishijima et al.*, 2009]. This absence of a significant change in interhemispheric difference over two decades suggests that the relative source strengths of $N_2O$ have remained constant between two hemispheres, with 60–70% coming from the Northern Hemisphere [*Butler et al.*, 1989].

[27] As shown in Figure 5b, mean values of the $N_2O$ mixing ratios observed at the AGAGE stations http://agage.eas.gatech.edu/index.htm) are consistent with the measurements during the AMT-7 cruise, confirming the background observations in the marine boundary layer. The mean values were obtained by averaging the $N_2O$ mixing ratios observed between 3 days before and after the date the AMT-7 cruise crossed the latitudes of the individual stations.

[28] $N_2O$ mixing ratios in the Northern Hemisphere increased slightly heading south toward the ITCZ (0.007 ± 0.003 ppb per degree latitude). This could be attributed to the large emissions of $N_2O$ from tropical and agricultural soils that are concentrated in the northern part of the tropics. Crossing the ITCZ, the $N_2O$ mixing ratios gradually decreased until 10°S. Afterward, the $N_2O$ mixing ratios remained constant until the air mass from the Antarctic circumpolar region was encountered (Table 1). Thus, between ~10°N and ~10°S seems to be a transition zone for $N_2O$ between the two hemispheres. The $N_2O$ mixing ratios in the high latitudes of the Southern Hemisphere (44°S to 52°S) appear to be slightly larger than those at low latitudes (~10°S to ~30°S). The reason is uncertain, but it could be due to the strong emissions from the Southern Ocean [*Nevison et al.*, 1995].

### 5.2. Variations in the Surface Mixed Layer of the Atlantic

[29] Dissolved $CH_4$ and $N_2O$ concentrations mirror SST in general, as temperature is the major parameter for gas solubility (Figures 6 and 7). Any departure from thermodynamic equilibrium of dissolved gases is useful in identifying sources or sinks of the gases, and to estimate gas fluxes across the air-water interface. The saturation anomaly ($\Delta g$) of a gas, $g$, is defined as the extent to which the dissolved concentration of the gas in seawater deviates from its mixing ratio in the overlying air,

$$\Delta g = \frac{x_g}{y_g} - 1 = SR - 1, \tag{4}$$

where $x_g$ and $y_g$ are the dry mixing ratios of the gas in air equilibrated with seawater and in the marine boundary layer, respectively, and $SR$ is the saturation ratio.

#### 5.2.1. Methane

[30] The dissolved $CH_4$ concentrations varied from 1.8 to 5 nmol $kg^{-1}$ and $\Delta CH_4$ from −0.03 to ~1.2 along the cruise track (Figure 6). High concentrations of up to 3.8 and 5.0 nmol $kg^{-1}$ were encountered in the coastal regions near the English Channel and the outflow of the Rio de la Plata, respectively. Extremely high $CH_4$ concentrations observed off the mouth of the Rio de la Plata are attributed to the influence of the outflow of muddy fresh water from the river, which seems to bring large amounts of dissolved $CH_4$ to the ocean, similar to other estuaries [*Bange et al.*, 1994]. In spite of the high dissolved $CH_4$ in the Rio de la Plata, the mean $\Delta CH_4$ for the coastal region over the Falkland continental shelf of 0.19 (±0.25) is virtually the same as that for the northern part of the English channel and the southern limb of the Celtic Sea of 0.26 (±0.18).

[31] Upwelling zones in the ocean are known to be source regions of $CH_4$, as a dissolved $CH_4$ maximum is often observed at or below the pycnocline [e.g., *Kelley and Jeffrey*, 2002]. In addition, the rich supply of nutrients in the water column below the euphotic zone stimulates biological activity in the mixed layer, which in turn enhan-

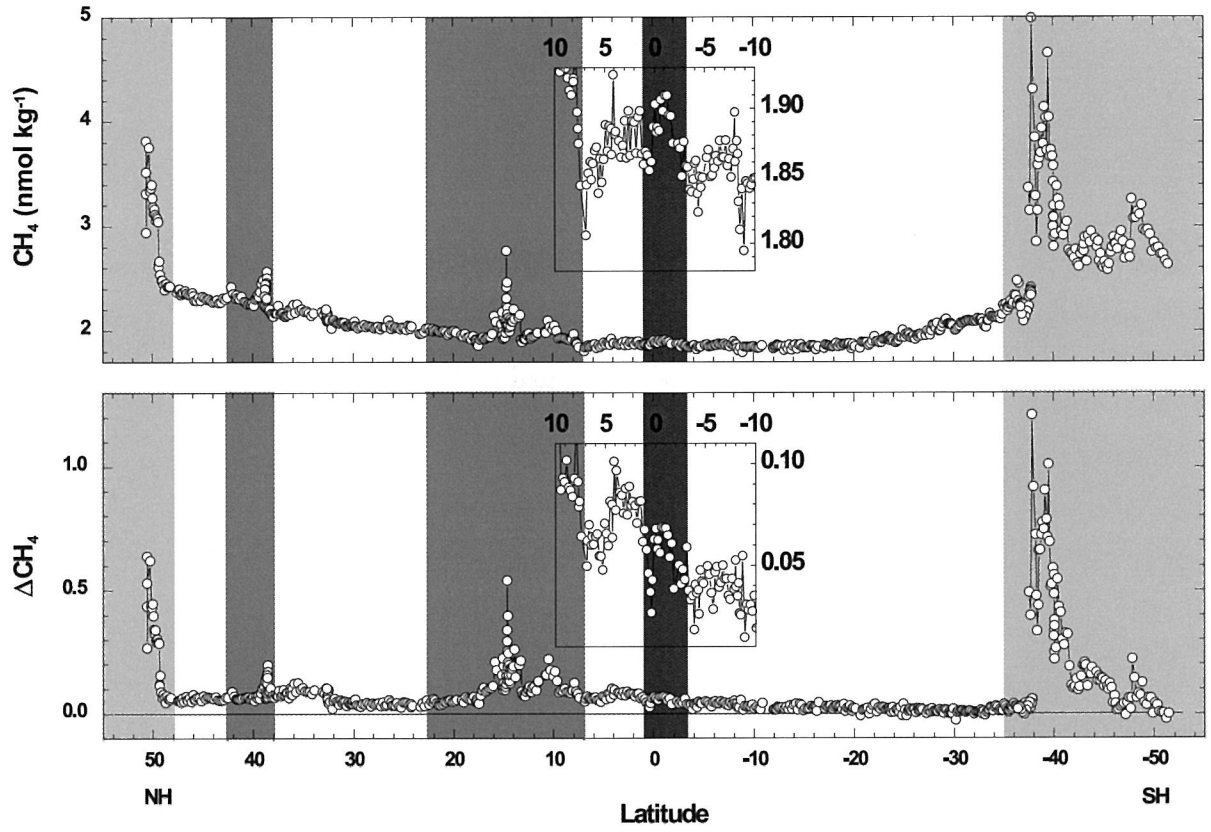


**Figure 6.** (top) Dissolved $CH_4$ concentrations and (bottom) their saturation anomalies ($\Delta CH_4$) along the cruise track. The inset is a scale-up of the parameters around the equatorial upwelling region. Different gray scales indicate regions characterized in Figure 4.

ces production of particulate material that forms microhabitats for methane-producing bacteria [*Karl and Tilbrook*, 1994; *Owens et al.*, 1991]. We observed an enhancement of $\Delta CH_4$ ($0.11 \pm 0.07$) in the coastal upwelling zone (Figure 6), although its magnitude is only about half of that in the coastal region ($0.20 \pm 0.24$). Nevertheless, the mean value is comparable to that found in the coastal upwelling region of the Arabian Sea (0.07–0.16) [*Bange et al.*, 1998]. *Conrad and Seiler* [1988] also encountered an increase of $CH_4$ in the coastal upwelling zone and in coastal regions in the Atlantic.

[32] $CH_4$ in the open ocean was only slightly supersaturated. Concentrations as low as ~1.8 nmol $kg^{-1}$ were observed at both the northern (7°N) and southern (9°S) edges of the equatorial upwelling zone, perhaps owing to high SST and low biological activity (Figures 4a and 4c). Slightly undersaturated or saturated waters with respect to the overlying atmospheric $CH_4$ were observed sporadically in the southern limb of the southern Atlantic subtropical gyre and near the Falkland Islands, although the number of observations of undersaturated waters (7 out of 721 points) is not significant. In contrast, the surface seawaters along the cruise track in the Northern Hemisphere were always supersaturated during the campaign, owing probably to the seasonal asymmetry of the radiative warming of the sea surface between the hemispheres. We did not observe significant elevation of the $CH_4$ concentration in the equatorial upwelling zone (see inset in Figure 6). $\Delta CH_4$ at the peak of the equatorial upwelling zone was merely 0.07, which is lower than the value in the adjacent waters at ~4°N, in contrast to what *Bates et al.* [1996] found in the Pacific upwelling region. This is likely due to the difference in SST between the two regions, as the dissolved $CH_4$ concentration in the equatorial upwelling zone is higher than, or similar to, that at ~4°N. We suspect that the high $\Delta CH_4$ at ~4°N originates from the upwelled waters at the African coast, which is also suggested by the enhancement of the dissolved $N_2O$ at the same location, and by vertical profiles of $N_2O$ in the water column (see section 5.2.2). While *Conrad and Seiler* [1988] observed a small increase of dissolved $CH_4$ in the equatorial upwelling zone during Jan/Feb of 1979, no distinct enhancement was found during Oct/Nov 1980, which is similar to our case.

### 5.2.2. Nitrous Oxide

[33] $N_2O$ is a product of denitrification or nitrification by bacteria in the ocean, although nitrification is likely to be the dominant process [*Cohen and Gordon*, 1978; *Dore et al.*, 1998; *Elkins et al.*, 1978; *Kim and Craig*, 1990; *Naqvi et al.*, 1998; *Nevison et al.*, 2003; *Yoshida et al.*, 1989]. Thus, a sharp peak in $N_2O$ concentration is usually observed beneath the euphotic zone in the ocean, anticorrelated with the dissolved $O_2$ profile [*Butler et al.*, 1989; *Kim and Craig*, 1990]. This high potential source of $N_2O$ is particularly pronounced in upwelling regions, as a large amount of $N_2O$

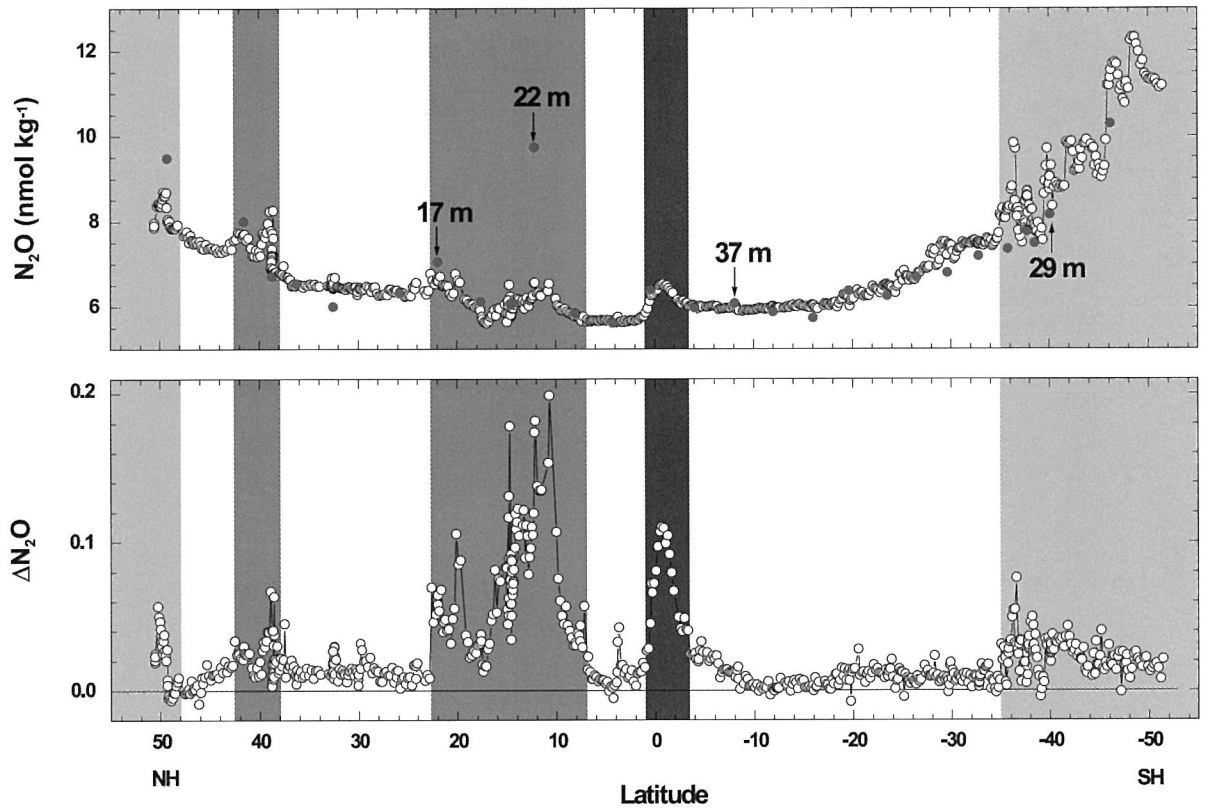


**Figure 7.** (top) Dissolved $N_2O$ concentrations and (bottom) their saturation anomalies ($\Delta N_2O$) along the cruise track. Different gray scales indicate regions characterized in Figure 4. The red circles on the top plot indicate discrete $N_2O$ measurements in surface waters collected from depths of 4–11 m. Seawater samples collected from depths > 11 m are designated by arrows with the depths marked above or below the arrow.

can be delivered to the surface by upwelling water [*Nevison et al.*, 2004]. In consequence, high $N_2O$ in surface waters often serves as an indicator for upwelling regions. As shown in Figure 7, elevated $\Delta N_2O$ was observed in the coastal and equatorial upwelling zones. In particular, $\Delta N_2O$ off the West African coast is 0.07(±0.04) on average. Such a large supersaturation off the West African coast has been reported before: *Oudot et al.* [2002] observed a $\Delta N_2O$ of 0.08 and *Walter et al.* [2004] observed up to 0.13. A large $\Delta N_2O$ of up to ~0.1 was also observed in the equatorial upwelling zone (the peak was near the equator) where enhancement of chl *a* and fluorescence was also observed (see Figure 4). A similar magnitude of $\Delta N_2O$ was also observed by *Walter et al.* [2004] in the Atlantic equatorial upwelling zone.

[34] The impact of upwelling water on supplying $N_2O$ to the surface is clearly represented by the vertical distribution in the water column along the cruise track (Figure 8); enhanced dissolved $N_2O$ (up to ~30 nmol kg$^{-1}$) was observed between ~25°N and ~8°S, where water masses of low temperature and salinity were encountered. In particular, the largest column content of dissolved $N_2O$ was observed offshore of Dakar (~14°N), where seawater temperature and salinity were low compared to the adjacent water column at the same depth, corroborating the upwelling off the West African coast as the source of high $\Delta N_2O$ at the surface. Another bulge of high dissolved $N_2O$ at ~70 m depth is located below the equatorial upwelling zone, where, again, a colder and less saline water mass was encountered.

[35] Agreement between discrete and continuous measurements of $N_2O$ demonstrates homogeneous $N_2O$ distribution in most of the surface mixed layer along the cruise track (Figure 7). At two stations, one a coastal region (50°N) and the other a coastal upwelling area (12°N), however, a substantial difference was found, probably owing to a shallow mixed layer.

[36] In contrast to $CH_4$, the coastal regions were not a significant source of $N_2O$ during the cruise. Of note is that $\Delta N_2O$ at the mouth of the Rio de la Plata is similar to values in other coastal regions. Also, the mean value of $\Delta N_2O$ of 0.023(±0.013) for the coastal region is not statistically different from that for the open ocean (0.014 ± 0.017), as seems to be the case for other oceans [*Bange et al.*, 1996a]. This might suggest that biological processes in the surface water contribute little to $N_2O$ production. Light penetration to the surface mixed layer, and high dissolved oxygen could inhibit the microbial production of $N_2O$ there [*Horrigan et al.*, 1981].

[37] The mean $\Delta N_2O$ of the open ocean (0.014 ± 0.017) agrees well with what was observed by *Butler et al.* [1989] (0.025), but is lower than the globally extrapolated value of 0.035 by *Nevison et al.* [1995]. Considering the rather

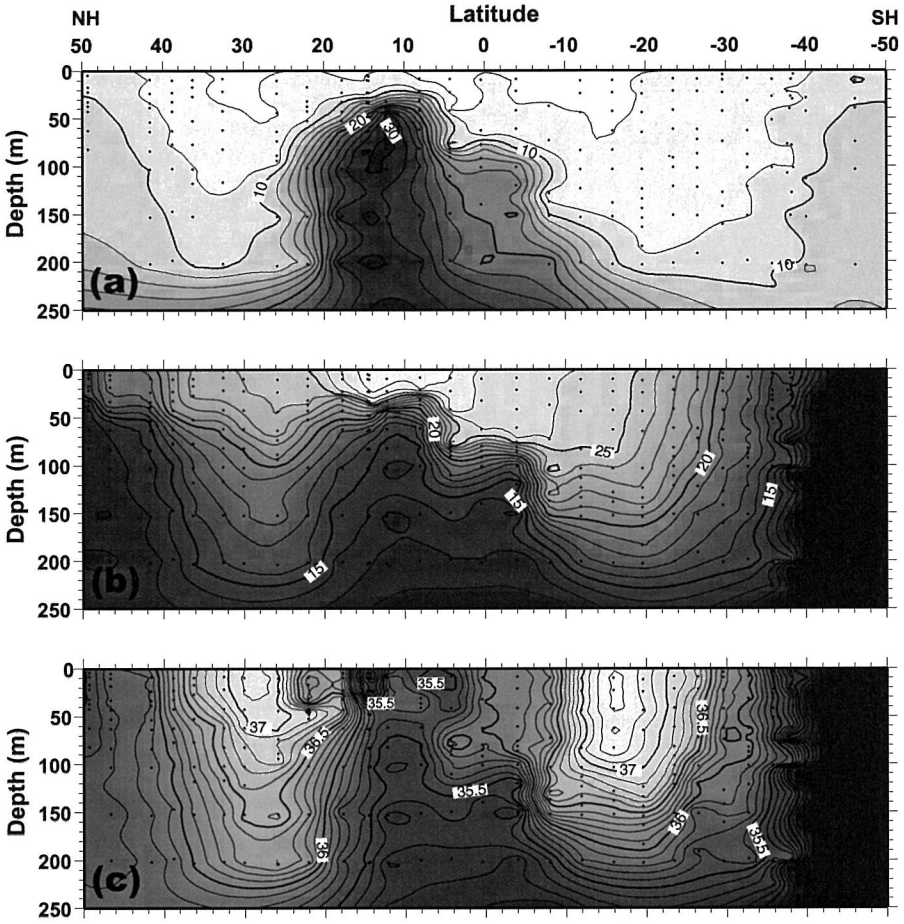


**Figure 8.** Vertical cross sections of (a) $N_2O$ concentration (nmol $kg^{-1}$), (b) seawater temperature (°C), and (c) salinity (‰) along the cruise track. Black dots represent sampling depth.

homogeneous distribution of $N_2O$ in the open ocean (see Figure 7), this suggests a lower mean surface concentration of $N_2O$ in the Atlantic than in the other oceans. Even though the limited spatial and seasonal coverage of the present study could bias the results, a lesser upwelling intensity and lower concentration of $N_2O$ in the subsurface water column in the Atlantic may play a role [*Nevison et al.*, 2003]. As discussed above, upwelling of subsurface waters is the largest source of $N_2O$ in the ocean. *Butler et al.* [1989] also ascribed the lower $\Delta N_2O$ observed during the SAGA II expedition in the Pacific to the suppressed equatorial upwelling that occurred during an El Niño event.

### 5.3. Emissions From the Ocean

[38] The flux (F) of a gas from the ocean can be calculated by multiplying the flux density ($j$) by the surface area ($A$),

$$F = jA. \tag{5}$$

The flux density is a product of the gas transfer velocity and the difference of gas concentrations between the surface seawater and the overlying atmosphere. We use the convention that a positive flux means emission from the oceans and a negative flux indicates absorption by the oceans. Since dissolved concentrations are interchangeable with partial pressure as given by Henry's law, the flux density can be given by

$$\begin{aligned} j &= k(C_w - LC_a) \\ &= kK_0 p_a \Delta g, \end{aligned} \tag{6}$$

where $k$ is a gas transfer velocity, $C_w$ and $C_a$ are the concentrations in the water and the overlying atmosphere respectively, $L$ is the Ostwald solubility coefficient, $K_0$ is the reciprocal of the Henry's law constant, $p_a$ is the atmospheric partial pressure, and $\Delta g$ indicates the saturation anomaly as defined by equation (4).

[39] Although numerous parameterizations of $k$ have been suggested, those by *Liss and Merlivat* [1986], *Wanninkhof* [1992], *Erickson* [1993], and *Nightingale et al.* [2000] have been widely used in the literature. The *Liss and Merlivat* [1986] model (hereinafter LM86) is based on experimental results from a lake and the laboratory. The *Wanninkhof* [1992] model (hereinafter W92) is simply fitted to the natural and bomb $^{14}C$ gas invasion rate with a long-term average of global wind speed. The *Erickson* [1993] model

**Table 2.** Parameterizations of Gas Transfer Velocity Applied for Calculation of $CH_4$ and $N_2O$ Fluxes[a]

| | Gas Transfer Velocity (cm $h^{-1}$) | Wind (m $s^{-1}$) |
|---|---|---|
| *Liss and Merlivat* [1986] | $k_g = 0.17U_{10}\left(\frac{Sc_g}{600}\right)^{-2/3}$ | $U_{10} \leq 3.6$ |
| | $k_g = (2.85U_{10} - 9.65)\left(\frac{Sc_g}{600}\right)^{-1/2}$ | $3.6 < U_{10} \leq 13$ |
| | $k_g = (5.9U_{10} - 49.3)\left(\frac{Sc_g}{600}\right)^{-1/2}$ | $U_{10} > 13$ |
| *Wanninkhof* [1992] | $k_g = 0.39U_{10}^2\left(\frac{Sc_g}{660}\right)^{-1/2}$ | Climatology |
| | $k_g = 0.31U_{10}^2\left(\frac{Sc_g}{660}\right)^{-1/2}$ | Shipboard |
| *Erickson* [1993] | $k_g = (5(1 - W) - 1300W)\left(\frac{Sc_g}{Sc_{Rn}}\right)^{-2/3}$ | $U_{20} < 3.6$ |
| | $k_g = (5(1 - W) - 1300W)\left(\frac{Sc_g}{Sc_{Rn}}\right)^{-1/2}$ | $U_{20} \geq 3.6$ |
| *Nightingale et al.* [2000] | $k_g = (0.222U_{10} + 0.333)U_{10}\left(\frac{Sc_g}{600}\right)^{-1/2}$ | |

[a] $U_{10}$ and $U_{20}$ indicate the wind speed at 10 and 20 m height, respectively; $k$ is gas transfer velocity; $Sc_g$ is the Schmidt number of a gas measured at a given temperature and salinity of seawater; and $W$ is the fraction of whitecap coverage and is a function of wind speed at 20 m asl, sea surface temperature, overlying air temperature, and relative humidity. *Erickson* [1993] calculated the Schmidt numbers for $CO_2$ and Rn using his own empirical equations ($Sc_{CO_2}$(E) and $Sc_{Rn}$(E)), but the results from these relationships are significantly different from data of *Jähne et al.* [1987] (e.g., the Erickson $Sc$(E) for $CO_2$ and Rn at 20°C and 35‰ are 565.3 and 869.3, whereas the values of Sc for $CO_2$ and Rn from the latter are 663.7 and 977.2 under the same conditions). Although the absolute values are significantly different, the ratio of $Sc_{CO_2}$(E)/$Sc_{Rn}$(E) is only 5% lower than $Sc_{CO_2}/Sc_{Rn}$. This difference results in a 2% decrease of the gas transfer velocity from *Erickson* [1993] when using our algorithm.

(hereinafter E93) extends the white cap model of *Monahan and Spillane* [1984] by differentiating the efficiency of the transfer velocity between whitecap and nonwhitecap regions and by involving the thermal stability of the air-sea interface to define the whitecap coverage. *Nightingale et al.* [2000] determined the values of $k$ on the basis of triple tracer experiments using bacterial spores, $SF_6$, and $^3He$ in the coastal region, and parameterized $k$ with wind speed in situ. These four parameterizations differ by a factor of ~2, but all capture the higher-order dependence of the $k$ on wind speed. We chose them for this study because they bracket the available data and are used for comparing our gas flux estimates with previous values. In Table 2 these four models and the normalization of the Schmidt number ($Sc$) are summarized.

[40] The shipboard wind speeds were measured along the cruise track using an anemometer that was mounted on the foremast at ~20 m asl. These apparent wind speeds were corrected to true wind speeds according to the algorithm by *Smith et al.* [1999] and then adjusted to a height of 10 m assuming a logarithmic profile of wind speed [*Kraus and Businger*, 1994].

[41] Because global extrapolations of gas flux are often based on climatological data, it is important to compare gas fluxes calculated from shipboard data against long-term mean values from climatological compilations. For this, we chose COADS/CMR-5 to obtain wind speeds, SST and SSS, SAT, and RH. The wind speeds from COADS/CMR-5 are averages at the height of an anemometer on shipboard (approximately 19.5 m), and it was assumed that they are representative of 20 m above sea level. The observations for SAT, SST, and SSS for shipboard and the COADS/CMR-5 data sets are similar (Figures 2 and 4). However, COADS/CMR-5 wind speed did not reproduce the variability of our shipboard wind speed. Nonetheless the mean wind speeds are similar to each other; the mean values from our shipboard observation and COADS/CMR-5 were 6.8(±3.7) m $s^{-1}$ and 6.4(±0.9) m $s^{-1}$, respectively.

[42] Flux densities of the gases were determined from equation (6) using calculated values of $k$ and solubility, and the values of partial pressures from the surface seawater and the overlying atmosphere measured underway. We then computed the mean flux densities for the gases in the open ocean, coastal region, and coastal upwelling zone. Assuming that these mean values of the flux densities are representative for each region, the regional and global fluxes of $CH_4$ and $N_2O$ are evaluated in Tables 3a and 3b. The global flux for each gas depends on the model of $k$ and wind speed used since it was assumed that the saturation anomalies and the partial pressures (or fugacity) were invariable temporally. While the mean climatological wind speed is similar to the mean shipboard wind speed on a global scale, the mean flux using the climatological wind data is as much as ~40% lower, suggesting that the gas flux at high wind speed significantly affects the estimation of the global flux from the ocean. Using COADS/CMR-5 wind data, the best estimates of global $CH_4$ emissions from the open ocean and coastal regions are the same value of 0.4 Tg $a^{-1}$, while $N_2O$ emitted from the open ocean is three times higher than from the coastal region.

## 6. Discussion

### 6.1. $\Delta CH_4$ in the Open Ocean

[43] The open ocean has low biological activity and consists of relatively homogeneous ecological settings. This is reflected by less variation of $\Delta CH_4$ in the open ocean than in other regions along the cruise track (Figure 6). In spite of the homogeneity of the open ocean, our mean $\Delta CH_4$ (0.04 ± 0.03) turns out to be far lower than the previous estimation of 0.2–0.3 by *Bange et al.* [1994], *Lambert and Schmidt* [1993] and *Ehhalt* [1974] (Table 4). A large discrepancy between measurements appears even in the Atlantic; *Oudot et al.* [2002] observed a $\Delta CH_4$ in the equatorial Atlantic of 0.19(±0.06) during January–March of 1993 and *Robinson et al.* [2006] of 0.50(±0.40) for 2003 in the southern Atlantic. In contrast, *Conrad and Seiler* [1988] observed a $\Delta CH_4$ of less than 0.10 in the open ocean, not much different from our measurements. Furthermore, *Bates et al.* [1996] observed $\Delta CH_4$ in the Pacific as 0.03 on average, which is the same value as we obtained in the Atlantic. What causes such a large discrepancy between measurements in the open ocean, in spite of its homogeneous ecological properties, is an open question. One potential candidate would be the methodology by which dissolved $CH_4$ is extracted (H. W. Bange, personal communication, 2000). While *Swinnerton and Linnenbom* [1967], *Oudot et al.* [2002], and *Robinson et al.* [2006] used a purge-and-trap method, *Conrad and Seiler* [1988], *Bates et al.* [1996], and we employed a dynamic equilibrium method. The method used by *Bates et al.* [1996] is exactly the same as ours. Bacterial $CH_4$ production in the microniches of oceanic particles, where an anoxic environment forms, is responsible for sustaining the supersaturation of

**Table 3a.** Regional and Global Fluxes of $CH_4$, Estimated From the AMT-7 Expedition Using in Situ and Climatological Data

| | | | Shipboard | | | | | | | Climatology | | | | | | |
|---|---|---|---|---|---|---|---|---|---|---|---|---|---|---|---|---|
| | | | | Flux[a] (Tg $a^{-1}$) | | | | | Mean Flux Fraction (%) | | Flux[a] (Tg $a^{-1}$) | | | | | Mean Flux Fraction (%) |
| | Area ($\times 10^6$ $km^2$) | $\Delta CH_4$ | Wind (m $s^{-1}$) | LM86 | W92 | E93 | N00 | Mean | | Wind (m $s^{-1}$) | LM86 | W92 | E93 | N00 | Mean | |
| Coastal region | 48.4 | 0.20 | 11 | 0.50 | 0.91 | 0.98 | 0.70 | 0.77 | 63 | 7.4 | 0.29 | 0.58 | 0.34 | 0.38 | 0.40 | 49 |
| Coastal upwelling | 0.4 | 0.11 | 4.8 | $4.9 \times 10^{-4}$ | $9.5 \times 10^{-4}$ | $1.2 \times 10^{-3}$ | $8.2 \times 10^{-4}$ | $8.7 \times 10^{-4}$ | 0.1 | 5.4 | $5.9 \times 10^{-4}$ | $1.3 \times 10^{-3}$ | $1.1 \times 10^{-3}$ | $9.2 \times 10^{-4}$ | $9.7 \times 10^{-4}$ | 0.1 |
| Open ocean | 313.3 | 0.040 | 6.2 | 0.32 | 0.55 | 0.52 | 0.45 | 0.46 | 37 | 6.5 | 0.29 | 0.58 | 0.38 | 0.39 | 0.41 | 51 |
| Global | 362 | 0.062[b] | 6.8[b] | 0.82 | 1.5 | 1.5 | 1.2 | 1.2 | | 6.6[b] | 0.59 | 1.2 | 0.72 | 0.76 | 0.81 | |

[a]LM86, W92, E93, and N00 denote gas transfer parameterizations of *Liss and Merlivat* [1986], *Wanninkhof* [1992], *Erickson* [1993], and *Nightingale et al.* [2000], respectively.
[b]Global saturation anomaly and wind speed are area-weighted mean values.

**Table 3b.** Regional and Global Fluxes of $N_2O$ Estimated From the AMT-7 Expedition Using in Situ and Climatological Data

| | | | Shipboard | | | | | | | Climatology | | | | | | |
|---|---|---|---|---|---|---|---|---|---|---|---|---|---|---|---|---|
| | | | | Flux[a] (Tg N $a^{-1}$) | | | | | Mean Flux Fraction (%) | | Flux[a] (Tg N $a^{-1}$) | | | | | Mean Flux Fraction (%) |
| | Area ($\times 10^6$ $km^2$) | $\Delta N_2O$ | Wind (m $s^{-1}$) | LM86 | W92 | E93 | N00 | Mean | | Wind (m $s^{-1}$) | LM86 | W92 | E93 | N00 | Mean | |
| Coastal Region | 48.4 | 0.023 | 11 | 0.44 | 0.80 | 0.88 | 0.62 | 0.68 | 43 | 7.4 | 0.23 | 0.45 | 0.25 | 0.29 | 0.31 | 26 |
| Coastal Upwelling | 0.4 | 0.057 | 4.9 | $1.5 \times 10^{-3}$ | $2.8 \times 10^{-3}$ | $3.5 \times 10^{-3}$ | $2.4 \times 10^{-3}$ | $2.6 \times 10^{-3}$ | 0.2 | 5.5 | $1.7 \times 10^{-3}$ | $3.7 \times 10^{-3}$ | $3.0 \times 10^{-3}$ | $2.6 \times 10^{-3}$ | $2.8 \times 10^{-3}$ | 0.2 |
| Open Ocean | 313.3 | 0.014 | 6.2 | 0.64 | 1.1 | 1.0 | 0.89 | 0.90 | 57 | 6.4 | 0.64 | 1.3 | 0.81 | 0.84 | 0.89 | 74 |
| Global | 362 | 0.015[b] | 6.8[b] | 1.1 | 1.9 | 1.9 | 1.5 | 1.6 | | 6.6[b] | 0.87 | 1.7 | 1.1 | 1.1 | 1.2 | |

[a]LM86, W92, E93, and N00 denote gas transfer parameterizations of *Liss and Merlivat* [1986], *Wanninkhof* [1992], *Erickson* [1993], and *Nightingale et al.* [2000], respectively.
[b]Global saturation anomaly and wind speed are area-weighted mean values.

**Table 4.** Comparison of the Parameters Which are Involved in the Determination of $CH_4$ Emission From the Ocean

| Literature | $j$ (mg m$^{-2}$ a$^{-1}$) | SST (°C) | $U_{10}$[a] (m s$^{-1}$) | $k$ (cm h$^{-1}$) | $K_0$[b] (mmol L$^{-1}$ atm$^{-1}$) | $x$CH$_4$ ($\mu$mol mol$^{-1}$) | $\Delta$CH$_4$ | Area ($\times 10^6$ km$^2$) |
|---|---|---|---|---|---|---|---|---|
| *Ehhalt* [1974] | | | | | | | | |
| Open ocean | 9–15 | 28[c] | 8–11 | 14–24 | 1.082 | 1.35 | 0.3 | 361 |
| Coastal | (50–100) × $10^3$ | 28[c] | 8–11 | 14–24 | 1.082 | 1.35 | 1700–2000 | 1.4[d] |
| *Lambert and Schmidt* [1993] | | | | | | | | |
| Open ocean | 10 | 20 | 8 | 13 | 1.24 | 1.55 | 0.3 | 360 |
| Coastal | 250 | 20 | 13 | 26 | 1.24 | 1.55 | 3.6 | 25 |
| *Bange et al.* [1994] | | | | | | | | |
| Open ocean | 9–15 | 13 | 9 | 13–21 | 1.43 | 1.7 | 0.2 | 307 |
| Coastal[e] | 140–230 | 13 | 9 | 13–21 | 1.43 | 1.7 | 3.2 | 57 |
| *Conrad and Seiler* [1988] | | | | | | | | |
| Open ocean and Coastal | 1–17 | 15–25 | 7–15 | 9–44 | 1.14–1.37 | 1.6 | 0.1 ± 0.05 | 361 |
| *Bates et al.* [1996] | | | | | | | | |
| Open ocean | 0.6–1.2 | 20 | 6.9 | 9–18 | 1.24 | 1.28 | 0.03 | 342.5 |
| This study | | | | | | | | |
| Open ocean | 1–2 | 23 ± 3 | 6.5 ± 0.7 | 8.5–17 | 1.16 ± 0.06 | 1.76 | 0.040 | 313.3 |
| Coastal | 6–12 | 13 ± 5 | 7 ± 1 | 9–17 | 1.5 ± 0.1 | 1.76 | 0.2 | 48.7 |

[a]Unless stated in the literature, the value was calculated from $k$ using *Liss and Merlivat* [1986] parameterization.
[b]Solubility was calculated by *Wiesenburg and Guinasso* [1979] at a given SST and 35‰.
[c]SST was calculated from the given diffusion coefficient.
[d]The effective coastal area in which $CH_4$ is emitted is assumed to be 1–10% of coastal region.
[e]This is considered as shelf regions by *Bange et al.* [1994].

the surface water [*Holmes et al.*, 2000; *Karl and Tilbrook*, 1994]. A recent result from laboratory experiments shows production of $CH_4$ by aerobic decomposition of methylphosphonate under conditions of low phosphate [*Karl et al.*, 2008]. This process could happen in particles as well. Since purge-and-trap methods force dissolved gases to be completely extracted, even the $CH_4$ in the particles could be collected during the extraction period, leading to a higher concentration than would occur in the water column. In future work, it would be worthwhile to investigate the possibility of differences in the determination of dissolved $CH_4$ in the open ocean due to the different methods applied.

### 6.2. Temporal Variation of $\Delta CH_4$ in the Atlantic

[44] The mean $\Delta CH_4$ during the AMT-7 cruise was estimated to be 0.09 (±0.14) using 721 observations. This mean value is the same that *Conrad and Seiler* [1988] estimated from measurements in the Atlantic about 20 years ago. We suspect that the regional variation of dissolved $CH_4$ concentrations in the Atlantic has not significantly changed during the 20 years from 1979 to 1998. *Bates et al.* [1996] found the $\Delta CH_4$ to remain steady in the North Pacific Ocean over a five year interval. It is noteworthy that the dissolved $CH_4$ in the Atlantic has kept up with the atmospheric growth rate of ~8.9 ppb a$^{-1}$ [*Dlugokencky et al.*, 1998] with the same saturation anomaly. To sustain the same saturation anomaly, an additional source, or an apparent increase of dissolved gas is required. As there is no evidence for an increase of $CH_4$ sources in the surface water, for example, biological activity, or of a long-term variation of ocean circulation, we believe that measurements of the same saturation anomaly in the Atlantic must originate from factors other than continual addition of $CH_4$ in the surface water.

[45] *Bates et al.* [1996] numerated several factors by which the saturation ratio of $CH_4$ could be changed. Among them, the seasonal variation of SST is a key parameter controlling the $\Delta CH_4$ in the extratropical open ocean and equatorial upwelling in the tropical region. But seasonal variations in dissolved $CH_4$ due to the rise and fall of SST effectively cancel out in the mean value, unless there is an overall trend of warming SST. Thus, one could attribute the additional source to the warming SST during the past 20 years, which forces the solubility to decrease. Since the warming SST does not change the content of dissolved $CH_4$, but rather solubility, the following simple equation can be derived from Henry's law (See Appendix for the derivation):

$$\frac{dT}{dt} = -\frac{\Delta CH_4}{x_{CH_4}} \left( \frac{d \ln L}{dT} \right)^{-1} \frac{dy_{CH_4}}{dt}, \tag{7}$$

where $T$ and $t$ denote SST and time, $x_{CH_4}$ and $y_{CH_4}$ are dry mixing ratios of dissolved and atmospheric $CH_4$, respectively, and $L$ is the Ostwald coefficient. Given the values of $\Delta CH_4$ = 0.1, $x_{CH_4}$ = 1760 ppb from *Conrad and Seiler* [1988], $d \ln L/dT$ = −0.01963 at 21°C, and $dy_{CH_4}/dt$ = 8.9 ppb a$^{-1}$ from *Dlugokencky et al.* [1998], the warming rate would be 0.026°C a$^{-1}$, which corresponds to a ~0.5°C increase of SST during the past 20 years. This simple estimation yields a value comparable to the increase of SST that IPCC [*Trenberth et al.*, 2007] reported. Although this might be fortuitous, it supports our speculation that the increase of SST plays a role in maintaining the supersaturation of $CH_4$ in the Atlantic.

### 6.3. Global Emission of $CH_4$ From the Ocean

[46] $CH_4$ emission from the ocean has been long accepted as being ~10 Tg a$^{-1}$, a value which is ~10 times larger than that estimated in the present study using climatological wind data (Table 5). The first assessment report by IPCC was published in 1990 [*IPCC*, 1990], and the estimated value of the $CH_4$ source strength of the ocean has since changed little in subsequent IPCC reports. The first and

**Table 5.** Global Emissions of $CH_4$ From the Ocean[a]

| Reference | Range[b] | Most Likely | Remark |
|---|---|---|---|
| | | *Basin-Wide Observations* | |
| This study | 0.6–1.2 | 0.8 | estimate based on data from the Atlantic |
| *Conrad and Seiler* [1988] | 0.3–3 | 1.5 | estimate based on data from the Atlantic |
| *Bates et al.* [1996] | 0.2–0.6 | 0.4 | estimate based on data from the Pacific open ocean |
| | | *IPCC Reports* | |
| *IPCC* [1990] | 5–20 | 10 | refers to work of *Cicerone and Oremland* [1988] which is based on work of *Ehhalt* [1974] |
| *IPCC* [1992] | 5–20 | 10 | refers to work of *IPCC* [1990] |
| *IPCC* [1995] | 5–50 | 10 | refers to work of *IPCC* [1990] and *Lambert and Schmidt* [1993] |
| *IPCC* [1996] | 5–50 | 10 | refers to work of *IPCC* [1995] |
| *IPCC* [2001] | | | |
| *Fung et al.* [1991] | | 10 | refers to work of *Ehhalt* [1974] |
| *Lelieveld et al.* [1998] | 5–15 | 10 | no literature citation |
| *Houweling et al.* [1999] | 5–25 | 15 | refers to work of *Lambert and Schmidt* [1993], *Lelieveld et al.* [1998], and its own model results |
| *IPCC* [2007] | | | |
| *Houweling et al.* [2000] | 5–25 | 15 | refers to work of *Lelieveld et al.* [1998] and *Houweling et al.* [1999] |
| *Wuebbles and Hayhoe* [2002] | | 4 | refers to work of *Khalil* [2000] which is based on work of *Lambert and Schmidt* [1993] |
| | | *Compilation of Data* | |
| *Ehhalt* [1974] | | | |
| Open ocean | 4–6.7 | | refers to work of *Swinnerton and Linnenbom* [1967] and R. A. Lamontagne et al. (1973)[c] |
| Coastal | 0.7–14 | | speculation |
| *Lambert and Schmidt* [1993] | | 10 | |
| Open ocean | | 3.6 | compilation of literature |
| Coastal | | 6.1 | speculation |
| *Bange et al.* [1994] | 11–18 | 15 | |
| Open ocean | 2.8–4.4 | 3.6 | compilation of literature |
| Coastal | 8.1–13.4 | 10.8 | compilation of literature |

[a]Emissions are in Tg $a^{-1}$.
[b]The range of values reflects mostly the uncertainties in $k$ parameterizations and saturation anomaly, $\Delta CH_4$. Exception are the estimates from this study, *Bates et al.* [1996], and *Bange et al.* [1994], which consider $k$ parameterizations as a major factor. See Table 4.
[c]Methane distribution in the world oceans, paper presented at International Symposium on Atmospheric Trace Gases, Commission on Atmospheric Chemistry and Global Pollution, Mainz, Germany, 1973.

second IPCC assessment reports [*IPCC*, 1990, 1996], the supplement report in 1992 [*IPCC*, 1995] and the special report in 1994 [*IPCC*, 1995] all ascribed the oceanic flux of $CH_4$ to the work by *Ehhalt* [1974], where the value was estimated on the basis of the measurements done by Swinnerton and coworkers [*Lamontagne et al.*, 1973; *Swinnerton and Linnenbom*, 1967] for the open ocean, combined with purely speculated emissions from the continental shelf. The special report in 1994 and the second IPCC assessment report expands the ceiling of the range to 50 Tg $a^{-1}$ with the same central value, taking into account the impact of shallow submarine gas seepage from the seafloor speculated by *Lambert and Schmidt* [1993]. The third [*Ehhalt et al.*, 2001] and fourth [*Denman et al.*, 2007] IPCC assessment reports do not explicitly state the oceanic source strength, but refer to the values in the literature, which again cited the same literature that the previous IPCC reports referred to. In conclusion, all IPCC reports essentially used the ocean source strength of $CH_4$ that was estimated by *Ehhalt* [1974].

[47] Since the publication of *Ehhalt* [1974], and before the present study, two basin-wide continuous measurements of $CH_4$, one in the Pacific [*Bates et al.*, 1996] and the other in the Atlantic [*Conrad and Seiler*, 1988], have been reported. In particular, the survey in the Pacific was conducted 5 times from 1987 to 1994 in various seasons, but in the open ocean. In the Atlantic, three surveys including the present study have been done. The estimates of $CH_4$ emissions from the ocean by these three studies are, however, far lower than the values in the series of IPCC reports (Table 5).

[48] There are several factors that could lead to this large discrepancy, such as differences in SST, SSS, wind speed, atmospheric mixing ratio of $CH_4$ ($xCH_4$), and $\Delta CH_4$ as listed in Table 4 (see equation (6)). The effect from differences in SST and SSS should be trivial as they only affect the solubility and the Schmidt number. An increase in $xCH_4$ of ~0.1 ppm merely changes the $CH_4$ flux by ~6%. Wind speed could be a considerable factor affecting the determination of $CH_4$ emissions from the ocean. Since $k$ increases exponentially with the increase of wind speed for most of the parameterizations, a small change in mean global wind speed induces a large increase in $k$, thus in the global emission rate. As *Nevison et al.* [1995] demonstrated by a sensitivity test, a 20% change in wind speed causes a 40~50% change in global flux; $k$ would vary as much as a factor of 2 depending on which parameterization is chosen. Yet obviously, none of these factors can account for an order-of-magnitude difference.

**Table 6.** Global Emissions of $N_2O$ in Tg N $a^{-1}$ From the Ocean

| Reference | Range | Most Likely | Remark |
|---|---|---|---|
| | | *Basin-Wide Observations* | |
| This study | 0.9–1.7 | 1.2 | estimate based on data from the Atlantic |
| *Butler et al.* [1989] | | 1.4 | estimate based on data from the Pacific |
| *Nevison et al.* [1995] | 1.2–6.8 | 4 | estimate based on data from the world oceans |
| | | *IPCC Reports* | |
| *IPCC* [1990] | 1.4–2.6 | | refers to work of *Butler et al.* [1989] |
| *IPCC* [1992] | 1.4–2.6 | | refers to work of *IPCC* [1990] |
| *IPCC* [1995] | 1–5 | 3 | accounts for strong emission from the upwelling regions |
| *IPCC* [1996] | | 3 | refers to work of *IPCC* [1995] |
| *IPCC* [2001] | | | |
| *Mosier et al.* [1998] and *Kroeze et al.* [1999] | 1–5 | 3 | no literature citation |
| *Olivier et al.* [1998] | 2.8–5.7 | 3.6 | refers to work of *Bouwman and Taylor* [1996] which is based on work of *Nevison et al.* [1995] |
| *IPCC* [2007] | 1.8–5.8 | 3.8 | refers to work of *Nevison et al.* [2003; 2004] which are essentially based on work of *Nevison et al.* [1995] |
| | | *Compilation of Data* | |
| *Bange et al.* [1996a] | 7–11 | | compilation of literature |
| Open ocean | 2.7–4.4 | | |
| Coastal | 4.3–6.7 | | |
| | | *Model Simulation* | |
| *Suntharalingam and Sarmiento* [2000] | 2.7–8 | 3.8 | based on a biogeochemical model in the water column |

[49] Consequently, the difference in mean $\Delta CH_4$ must be the key factor that accounts for such a large discrepancy in $CH_4$ flux from the ocean. The estimate of $\Delta CH_4$ in the open ocean by *Ehhalt* [1974] is ~8–10 times larger than the value estimated by *Bates et al.* [1996] and in this study (Table 4). Given the fairly homogeneous distribution of $CH_4$ in surface seawater and the lack of change in $\Delta CH_4$ with time in the open ocean (see section 6.1), the value of $\Delta CH_4$ adopted by *Ehhalt* [1974] appears to be biased by the experimental technique used by Swinnerton and coworkers [*Lamontagne et al.*, 1973; *Swinnerton and Linnenbom*, 1967], leading to an overestimation in the emission of $CH_4$ from the open ocean by an order of magnitude. For the same reasons, *Bange et al.* [1994] and *Lambert and Schmidt* [1993] obtained similar emission rates of $CH_4$ from the open ocean.

[50] Estimates of $\Delta CH_4$ for coastal regions are notoriously difficult because of variability and undersampling, and we feel that recent measurements may also force estimated fluxes from coastal regions to be revised downward. For the estimates of $\Delta CH_4$ in coastal regions, there is an even larger discrepancy between the estimates by *Ehhalt* [1974] and the present study. Because of the highly heterogeneous distribution of dissolved $CH_4$ in coastal regions, extrapolation of a few measurements to the global scale may lead to a bias in a global estimation. To avoid this, *Bange et al.* [1994] compiled data from the literature and estimated $\Delta CH_4$ for the coastal regions, including the estuarine areas, as 3.2, which is ~16 times larger than the value we estimated. The estimate by *Bange et al.* [1994], however, seems to be biased to the upper bound, according to recent observations in various coastal regions. For example, in estimating $\Delta CH_4$ for the coastal regions, *Bange et al.* [1994] assumed that $\Delta CH_4$ is ~26 in the Sea of Okhotsk, referring to the measurements by *Lammers et al.* [1995]. Recent measurements by *Yoshida et al.* [2004], however, show much lower $\Delta CH_4$ values of ~0.6. In addition, *Rehder and Suess* [2001] observed that $\Delta CH_4$ was 0.10 – 0.15 in most of the western coastal regions of the Pacific, though sporadic high values were encountered near the Honshu coast and the South China Sea, yielding an area-weighted mean $\Delta CH_4$ value of ~0.3. *Zhang et al.* [2004] also observed a conservative $\Delta CH_4$ value of 0.3(±0.2) in the East China Sea and the Yellow Sea. These $\Delta CH_4$ values are far lower than the $\Delta CH_4$ value of 1.4 that *Bange et al.* [1994] adopted for the coastal region of the Pacific. *Bange et al.* [1998] also observed $\Delta CH_4$ of the Arabian Sea to be as low as 0.03–0.16. Therefore, the coastal region worldwide does not seem to be as highly supersaturated as *Bange et al.* [1994] estimated. To the contrary, the recent observations of $\Delta CH_4$ described above support the value we estimated from the Atlantic coastal region, which strongly suggests our estimate of $CH_4$ emission from the ocean as being correct. We feel that reconsideration of the accepted oceanic fluxes may be needed in light of this reinterpretation of the coastal fluxes and recent evidence of the differences in the instrumental determination of $\Delta CH_4$.

### 6.4. Global Emission of $N_2O$ From the Ocean

[51] The estimated $N_2O$ emissions from the ocean range from 0.9 to 1.7 Tg N $a^{-1}$ in the present study (Table 6), which is somewhat lower than that estimated by the recent IPCC report [*IPCC*, 2007]. This is due largely to the lower $\Delta N_2O$ in the Atlantic than in the other oceans (see section 5.2.2). The third and fourth IPCC reports [*Denman et al.*, 2007; *Ehhalt et al.*, 2001] are in principle based on the results of *Nevison et al.* [1995], who estimated the $\Delta N_2O$ in the world oceans as 0.035, which is 2.3 times larger than the value observed in the Atlantic in the present study. *Nevison et al.* [1995] indicate that $\Delta N_2O$ in the surface waters of the

Pacific and the Indian Oceans is larger than that in the Atlantic owing to large upwelling regions in the northern Indian Ocean and Arabian Sea and in the tropical Pacific. This trend may be associated with the ventilation of deep waters in the world's oceans as well [*Bange and Andreae*, 1999] which pushes deep water to the surface in upwelling regions. As shown in Figure 8 and extensively in other studies [e.g., *Nevison et al.*, 2003], the $N_2O$ content in surface waters is strongly linked to the upwelling of subsurface waters in which $N_2O$ is produced by microbial activity. Therefore, the large difference in $\Delta N_2O$ in the open ocean upwelling regions is a significant factor in determining the $N_2O$ source strength of the ocean. This also explains the relatively low $N_2O$ emission from the ocean estimated by *Butler et al.* [1989], as they obtained lower saturation anomalies of 0.025 during an El Niño year due to the suppressed upwelling in the equatorial Pacific. Since the early IPCC reports [*IPCC*, 1990, 1992] were based on the observations by *Butler et al.* [1989], the oceanic source strength for atmospheric $N_2O$ given there was smaller than that in the later IPCC reports (Table 6).

[52] Upwelling at the coast also contributes to the supply of subsurface dissolved $N_2O$. As indicated in section 5.2.2, the saturation anomalies in the northwest African coastal upwelling zone are comparable to or, in some areas, even larger than that observed in the equatorial upwelling zone during the campaign (Figure 7). Nonetheless, our mean $\Delta N_2O$ of 0.057 in the coastal upwelling zone along the cruise track appears to be much lower than the values in other coastal upwelling zones (0.08–3.42) [*Bange et al.*, 1996a]. Recently, *Nevison et al.* [2004] estimated the $N_2O$ emission from coastal upwelling zones in the world as $\sim$0.05 Tg N $a^{-1}$ (by a gas transfer model). Given that they used global coastal upwelling areas of $1.76 \times 10^6$ $km^2$, that is $\sim$5 times larger than the area we have chosen in this study, and W92 model of $k$, $\Delta N_2O$ in the coastal upwelling zone should be no larger than $\sim$0.2 ( = 0.05 Tg N $a^{-1}$ $\div$ 0.0037 Tg N $a^{-1}$ $\times$ 0.4 $\times$ $10^6$ $km^2$ $\div$ $1.76 \times 10^6$ $km^2$ $\times$ 0.057) assuming that wind speed, SST, and SSS are similar to what we observed in the Atlantic coastal upwelling zones. Consequently, the emission rate of $N_2O$ in the coastal upwelling zone is probably not as large as *Bange et al.* [1996a] suggested. On the other hand, our estimation implies that the $\Delta N_2O$ in the coastal upwelling zones in the Atlantic is smaller than in other regions such as the Pacific West coasts of North and South America and the Arabian Sea [*Bange et al.*, 1996b; *Cornejo et al.*, 2007; *Nevison et al.*, 2004].

[53] To summarize, the content of dissolved $N_2O$ in upwelling waters, and the upwelling activity govern the $\Delta N_2O$ of surface waters in the ocean and, thus the emission strength of $N_2O$ to a large extent. Up to now, the best estimate of $N_2O$ emissions from the ocean is the work done by *Nevison et al.* [1995] ($\sim$4 Tg N $a^{-1}$), because of the wide coverage of ocean regions and time periods of the measurements, as well as the methodology by which the oceanic emissions are calculated. Addition of a considerable number of new data points from the Pacific, Indian, and Atlantic in work by *Nevison et al.* [2004] resulted in nearly the same estimate as that of *Nevison et al.* [1995]. However, as *Nevison et al.* [1995] admitted, the measurements applied for the estimation are biased to the summer season, which may lead to an overestimation. Thus, a reasonable range of global marine $N_2O$ flux estimates for future IPCC assessments may be 1.2–4.0 Tg N $a^{-1}$, where the lower bound is defined by our work and that of *Butler et al.* [1988], and the upper bound is based on the estimate of *Nevison et al.* [1995].

## 7. Summary and Conclusions

[54] 1. The saturation anomalies of $CH_4$ observed in the open ocean by different research groups differ widely. It is yet unknown what causes this discrepancy, but differences in methods used to collect dissolved $CH_4$ are a likely cause. The three basin-wide studies by *Bates et al.* [1996], *Conrad and Seiler* [1988], and this study, all of which used the same method to collect dissolved $CH_4$, indicate that the open ocean is supersaturated with respect to atmospheric $CH_4$ at a level of $\sim$0.04 on average. This is about an order of magnitude lower than the $\Delta CH_4$ value of 0.3 suggested by *Ehhalt* [1974], which was the basis for the oceanic $CH_4$ source estimate in the IPCC reports.

[55] 2. We estimate the $CH_4$ source strength of the ocean as 0.6–1.2 Tg $a^{-1}$, which is almost the same range obtained by the two basin-wide measurements in the Atlantic and in the Pacific, but is more than 10 times lower than the estimated value in the IPCC reports.

[56] 3. The basin-wide study by *Conrad and Seiler* [1988] and the present study in the Atlantic show the same $\Delta CH_4$ across an interval of 20 years, even though the atmospheric mixing ratio of $CH_4$ has increased continually during the same period. The same trend has been observed in the Pacific over an interval of 5 years. We speculate that global warming may be an important driver to maintain the same $\Delta CH_4$ in the ocean.

[57] 4. The global $N_2O$ emission from the ocean of 0.9–1.7 Tg N $a^{-1}$, estimated from Atlantic data in the present study, is $\sim$3 times lower than the value estimated from global ocean observations [*Nevison et al.*, 1995]. This implies that upwelling activities and/or the $N_2O$ content of subsurface waters in the open ocean and on the coast of the Atlantic are weaker than in the other oceans.

## Appendix A: Note on Warming SST and Constant Saturation Anomaly

[58] Assuming saturation anomaly, $\Delta g$, is constant while sea surface water is warming, the increment of the mixing ratio of dissolved gas can be given from the definition of $\Delta g$,

$$x = (\Delta g + 1)y, \tag{A1}$$

where $x$ and $y$ indicate the dry mixing ratio of dissolved and atmospheric gas, respectively.

[59] By differentiating (A1) with respect to time, $t$, we get

$$\frac{dx}{dt} = \Delta g \frac{dy}{dt}. \tag{A2}$$

Since increasing SST does not affect the concentration of dissolved gas but the mixing ratio, the derivative of

concentration with respect to time should be zero. Gas solubility can be defined as follows from Henry's law:

$$C = K_0 P x, \tag{A3}$$

where $C$ indicates concentration, $K_0$ is the reciprocal of the Henry's law constant, and $P$ is total pressure.

[60] By differentiating both sides of (A3) with respect to $t$, we obtain

$$\begin{aligned} \frac{dC}{dt} &= P\left(K_0 \frac{dx}{dt} + x\frac{dK_0}{dt}\right) \\ &= P\left(K_0 \Delta g \frac{dy}{dt} + x\frac{dK_0}{dT}\frac{dT}{dt}\right) \\ &= 0 \end{aligned} \tag{A4}$$

Hence

$$\frac{dT}{dt} = -\frac{\Delta g}{x}\left(\frac{d\ln K_0}{dT}\right)^{-1}\frac{dy}{dt}. \tag{A5}$$

Because the derivative of the natural logarithm of $K_0$ is the same as the derivative of the natural logarithm of the Ostwald coefficient ($L$), we get after substitution, the equation below:

$$\frac{dT}{dt} = -\frac{\Delta g}{x}\left(\frac{d\ln L}{dT}\right)^{-1}\frac{dy}{dt}. \tag{A6}$$

[61] **Acknowledgments.** We gratefully acknowledge the help of Jim Aiken, Douglas Trevitt, and other crew members of the RRS *James Clark Ross* in collecting samples. This research, funded by the Max Planck Society, has been done while T.S.R. was at the Max Planck Institute for Chemistry. T.S.R. is pleased to acknowledge the useful comments of D. R. Schink, R. A. Duce, and T. W. Andreae on an early version of the manuscript and the support from the Korean Science and Engineering Foundation (KOSEF) (grant R01-2007-000-20793-0) and Korean Polar Research Program (PP09040) for preparation of the manuscript.

## References

Aiken, J., N. Rees, S. Hooker, P. Holligan, A. Bale, D. Robins, G. Moore, R. Harris, and D. Pilgrim (2000), The Atlantic Meridional Transect: Overview and synthesis of data, *Prog. Oceanogr.*, *45*, 257–312, doi:10.1016/S0079-6611(00)00005-7.

Bange, H. W., and M. O. Andreae (1999), Nitrous oxide in the deep waters of the world's oceans, *Global Biogeochem. Cycles*, *13*(4), 1127–1135, doi:10.1029/1999GB900082.

Bange, H. W., U. H. Bartell, S. Rapsomanikis, and M. O. Andreae (1994), Methane in the Baltic and North seas and a reassessment of the marine emissions of methane, *Global Biogeochem. Cycles*, *8*(4), 465–480, doi:10.1029/94GB02181.

Bange, H. W., S. Rapsomanikis, and M. O. Andreae (1996a), Nitrous oxide in coastal waters, *Global Biogeochem. Cycles*, *10*(1), 197–207, doi:10.1029/95GB03834.

Bange, H. W., S. Rapsomanikis, and M. O. Andreae (1996b), Nitrous oxide emissions from the Arabian Sea, *Geophys. Res. Lett.*, *23*(22), 3175–3178, doi:10.1029/96GL03072.

Bange, H. W., R. Ramesh, S. Rapsomanikis, and M. O. Andreae (1998), Methane in surface waters of the Arabian Sea, *Geophys. Res. Lett.*, *25*(19), 3547–3550, doi:10.1029/98GL02710.

Bange, H. W., S. Rapsomanikis, and M. O. Andrea (2001), Nitrous oxide cycling in the Arabian Sea, *J. Geophys. Res.*, *106*(C1), 1053–1065, doi:10.1029/1999JC000284.

Bates, T. S., K. C. Kelly, J. E. Johnson, and R. H. Gammon (1996), A reevaluation of the open ocean source of methane to the atmosphere, *J. Geophys. Res.*, *101*(D3), 6953–6961, doi:10.1029/95JD03348.

Bekki, S., K. S. Law, and J. A. Pyle (1994), Effect of ozone depletion on atmospheric $CH_4$ and CO concentrations, *Nature*, *371*, 595–597, doi:10.1038/371595a0.

Bell, G. D., M. S. Halpert, C. F. Ropelewski, V. E. Kousky, A. V. Douglas, R. C. Schnell, and M. E. Gelman (1999), Climate assessment for 1998, *Bull. Am. Meteorol. Soc.*, *80*(5), 1040, doi:10.1175/1520-0477(1999)080<1040:CAF>2.0.CO;2.

Bouwman, A. F., and J. A. Taylor (1996), Testing high-resolution nitrous oxide emission estimates against observations using an atmospheric transport model, *Global Biogeochem. Cycles*, *10*(2), 307–318, doi:10.1029/96GB00191.

Butler, J. H., J. W. Elkins, C. M. Brunson, K. B. Egan, T. M. Thompson, T. J. Conway, and B. D. Hall (1988), Trace gases in and over the west Pacific and East Indian Ocean during the El Niño(Southern Oscillation event of 1987, *ERL ARL-16*, 104 pp., Air Resour. Lab., Silver Spring, Md.

Butler, J. H., J. W. Elkins, and T. M. Thompson (1989), Tropospheric and dissolved $N_2O$ of the west Pacific and east Indian oceans during the El Niño Southern Oscillation event of 1987, *J. Geophys. Res.*, *94*(D12), 14,865–14,877, doi:10.1029/JD094iD12p14865.

Butler, T. M., P. J. Rayner, I. Simmonds, and M. G. Lawrence (2005), Simultaneous mass balance inverse modeling of methane and carbon monoxide, *J. Geophys. Res.*, *110*, D21310, doi:10.1029/2005JD006071.

Chen, Y. H., and R. G. Prinn (2006), Estimation of atmospheric methane emissions between 1996 and 2001 using a three-dimensional global chemical transport model, *J. Geophys. Res.*, *111*, D10307, doi:10.1029/2005JD006058.

Cicerone, R. J., and R. S. Oremland (1988), Biogeochemical aspects of atmospheric methane, *Global Biogeochem. Cycles*, *2*(4), 299–327, doi:10.1029/GB002i004p00299.

Cohen, Y., and L. I. Gordon (1978), Nitrous oxide in the oxygen minimum of the eastern tropical North Pacific: Evidence for its consumption during denitrification and possible mechanisms for its production, *Deep Sea Res.*, *25*, 509–524, doi:10.1016/0146-6291(78)90640-9.

Conrad, R., and W. Seiler (1988), Methane and hydrogen in seawater (Atlantic Ocean), *Deep Sea Res., Part A*, *35*, 1903–1917, doi:10.1016/0198-0149(88)90116-1.

Cornejo, M., L. Farias, and M. Gallegos (2007), Seasonal cycle of $N_2O$ vertical distribution and air-sea fluxes over the continental shelf waters off central Chile (~36°S), *Prog. Oceanogr.*, *75*, 383–395, doi:10.1016/j.pocean.2007.08.018.

Crutzen, P. J. (1996), My life with $O_3$, $NO_x$, and other $YZO_x$ compounds (Nobel Lecture), *Angew. Chem. Int. Ed. Engl.*, *35*, 1758–1777, doi:10.1002/anie.199617581.

Denman, K. L., et al. (2007), Couplings between changes in the climate system and biogeochemistry, in *Climate Change 2007: The Physical Science Basis. Contribution of Working Group I to the Fourth Assessment Report of the Intergovernmental Panel on Climate Change*, edited by S. Solomon et al., pp. 501–587, Cambridge Univ. Press, Cambridge, U. K.

Dlugokencky, E. J., K. A. Masaire, P. M. Lang, P. P. Tans, L. P. Steele, and E. G. Nisbet (1994), A dramatic decrease in the growth rate of atmospheric methane in the Northern Hemisphere during 1992, *Geophys. Res. Lett.*, *21*(1), 45–48, doi:10.1029/93GL03070.

Dlugokencky, E. J., K. A. Masarie, P. M. Lang, and P. P. Tans (1998), Continuing decline in the growth rate of the atmospheric methane burden, *Nature*, *393*, 447–450, doi:10.1038/30934.

Dlugokencky, E. J., B. P. Walter, K. A. Masarie, P. M. Lang, and E. S. Kasischke (2001), Measurements of an anomalous global methane increase during 1998, *Geophys. Res. Lett.*, *28*(3), 499–502, doi:10.1029/2000GL012119.

Dore, J. E., B. N. Poppe, D. M. Karl, and F. J. Sansone (1998), A large source of atmospheric nitrous oxide from subtropical North Pacific surface waters, *Nature*, *396*, 63–66, doi:10.1038/23921.

Dutton, E. G., and J. R. Christy (1992), Solar radiative forcing at selected locations and evidence for global lower tropospheric cooling following the eruptions of El Chichon and Pinatubo, *Geophys. Res. Lett.*, *19*(23), 2313–2316, doi:10.1029/92GL02495.

Ehhalt, D. H. (1974), The atmospheric cycle of methane, *Tellus*, *26*, 58–70.

Ehhalt, D., et al. (2001), Atmospheric chemistry and greenhouse gases, in *Climate Change 2001: The Scientific Basis. Contribution of Working Group I to the Third Assessment Report of the Intergovernmental Panel on Climate Change*, edited by J. T. Houghton et al., pp. 239–287, Cambridge Univ. Press, Cambridge, U. K.

Elkins, J. W., S. C. Wofsy, M. B. McElroy, C. E. Kolb, and W. A. Kaplan (1978), Aquatic sources and sinks for nitrous oxide, *Nature*, *275*, 602–606, doi:10.1038/275602a0.

Erickson, D. J. I. (1993), Stability dependent theory for air-sea gas exchange, *J. Geophys. Res.*, *98*(C5), 8471–8488, doi:10.1029/93JC00039.

Fung, I., J. John, J. Lerner, E. Matthews, M. Prather, L. P. Steele, and P. J. Fraser (1991), Three-dimensional model synthesis of the global methane cycle, *J. Geophys. Res.*, *96*(D7), 13,033–13,065, doi:10.1029/91JD01247.

Hogan, K. B., and R. C. Harriss (1994), Comment on "A dramatic decrease in the growth rate of atmospheric methane in the Northern Hemisphere during 1992" by E. J. Dlugokencky et al., *Geophys. Res. Lett.*, *21*(22), 2445–2446, doi:10.1029/94GL02601.

Holmes, M. E., F. J. Sansone, T. M. Rust, and B. N. Popp (2000), Methane production, consumption, and air-sea exchange in the open ocean: An evaluation based on carbon isotopic ratios, *Global Biogeochem. Cycles*, *14*(1), 1–10, doi:10.1029/1999GB001209.

Horrigan, S. G., A. F. Carlucci, and P. M. Williams (1981), Light inhibition of nitrification in sea-surface films, *J. Mar. Res.*, *39*, 557–565.

Houweling, S., T. Kaminski, F. Dentener, J. Lelieveld, and M. Heimann (1999), Inverse modeling of methane sources and sinks using the adjoint of a global transport model, *J. Geophys. Res.*, *104*(D21), 26,137–26,160, doi:10.1029/1999JD900428.

Houweling, S., F. Dentener, J. Lelieveld, B. Walter, and E. Dlugokencky (2000), The modeling of tropospheric methane: How well can point measurements be reproduced by a global model?, *J. Geophys. Res.*, *105*(D7), 8981–9002, doi:10.1029/1999JD901149.

Intergovernmental Panel on Climate Change (1990), *Climate Change: The IPCC Scientific Assessment*, 364 pp., Cambridge Univ. Press, Cambridge, U. K.

Intergovernmental Panel on Climate Change (1992), *Climate Change 1992: The Supplementary Report to the IPCC Scientific Assessment*, 200 pp., Cambridge Univ. Press, Cambridge, U. K.

Intergovernmental Panel on Climate Change (1995), *Climate Change 1994: Radiative Forcing of Climate Change and An Evaluation of the IPCC IS92 Emission Scenarios*, 339 pp., Cambridge Univ. Press, Cambridge, U. K.

Intergovernmental Panel on Climate Change (1996), *Climate Change 1995 - The Science of Climate Change*, 572 pp., Cambridge Univ. Press, Cambridge, U. K.

Intergovernmental Panel on Climate Change (2001), *Climate Change 2001: The Scientific Basis, Contribution of Working Group I to the Third Assessment Report of the Intergovernmental Panel on Climate Change*, 881 pp., Cambridge Univ. Press, Cambridge, U. K.

Intergovernmental Panel on Climate Change (2007), *Climate Change 2007: The Physical Science Basis. Contribution of Working Group I to the Fourth Assessment Report of the Intergovernmental Panel on Climate Change*, 996 pp., Cambridge Univ. Press, Cambridge, U. K.

Ishijima, K., T. Nakazawa, and S. Aoki (2009), Variations of atmospheric nitrous oxide concentration in the northern and western Pacific, *Tellus, Ser. B*, *61*, 408–415.

Jähne, B., G. Heinz, and W. Dietrich (1987), Measurement of the diffusion coefficients of sparingly soluble gases in water, *J. Geophys. Res.*, *92*(C10), 10,767–10,776, doi:10.1029/JC092iC10p10767.

Johnson, J. E. (1999), Evaluation of a seawater equilibrator for shipboard analysis of dissolved oceanic trace gases, *Anal. Chim. Acta*, *395*, 119–132, doi:10.1016/S0003-2670(99)00361-X.

Karl, D. M., and B. D. Tilbrook (1994), Production and transport of methane in oceanic particulate organic matter, *Nature*, *368*, 732–734, doi:10.1038/368732a0.

Karl, D. M., L. Beversdorf, K. M. Björkman, M. J. Church, A. Martinez, and E. F. DeLong (2008), Aerobic production of methane in the sea, *Nat. Geosci.*, *1*, 473–478, doi:10.1038/ngeo234.

Kasischke, E. S., and L. P. Bruhwiler (2002), Emissions of carbon dioxide, carbon monoxide, and methane from boreal forest fires in 1998, *J. Geophys. Res.*, *107*, 8146, doi:10.1029/2001JD000461. [printed *108*(D1), 2003].

Kelley, C. A., and W. H. Jeffrey (2002), Dissolved methane concentration profiles and air-sea fluxes from 41°S to 27°N, *Global Biogeochem. Cycles*, *16*(3), 1040, doi:10.1029/2001GB001809.

Kettle, A. J., T. S. Rhee, M. von Hobe, A. Poulton, J. Aiken, and M. O. Andreae (2001), Assessing the flux of different volatile sulfur gases from the ocean to the atmosphere, *J. Geophys. Res.*, *106*(D11), 12,193–12,209, doi:10.1029/2000JD900630.

Khalil, M. A. K. (2000), Atmospheric methane: An introduction, in *Atmospheric Methane: Its Role in the Global Environment*, edited by M. A. K. Khalil, pp. 1–8, Springer, Berlin.

Kim, K.-R., and H. Craig (1990), Two-isotope characterization of $N_2O$ in the Pacific Ocean and constraints on its origin in deep water, *Nature*, *347*, 58–61, doi:10.1038/347058a0.

Kraus, E. B., and J. A. Businger (1994), *Atmosphere-Ocean Interaction*, 362 pp., Clarendon, New York.

Kroeze, C., A. Mosier, and L. Bouwman (1999), Closing the global $N_2O$ budget: A retrospective analysis 1500–1994, *Global Biogeochem. Cycles*, *13*(1), 1–8, doi:10.1029/1998GB900020.

Labitzke, K. (1994), Stratospheric temperature changes after the Pinatubo eruption, *J. Atmos. Terr. Phys.*, *56*(9), 1027–1034, doi:10.1016/0021-9169(94)90039-6.

Lambert, G., and S. Schmidt (1993), Reevaluation of the oceanic flux of methane: Uncertainties and long term variations, *Chemosphere*, *26*, 579–589, doi:10.1016/0045-6535(93)90443-9.

Lammers, S., E. Suess, M. N. Mansurov, and V. V. Anikiev (1995), Variations of atmospheric methane supply from the Sea of Okhotsk induced by the seasonal ice cover, *Global Biogeochem. Cycles*, *9*(3), 351–358, doi:10.1029/95GB01144.

Lamontagne, R. A., J. W. Swinnerton, V. J. Linnenbom, and W. D. Smith (1973), Methane concentrations in various marine environments, *J. Geophys. Res.*, *78*(24), 5317–5324, doi:10.1029/JC078i024p05317.

Langenfelds, R. L., R. J. Francey, B. C. Pak, L. P. Steele, J. Lloyd, C. M. Trudinger, and C. E. Allison (2002), Interannual growth rate variations of atmospheric $CO_2$ and its $\delta^{13}C$, $H_2$, $CH_4$, and CO between 1992 and 1999 linked to biomass burning, *Global Biogeochem. Cycles*, *16*(3), 1048, doi:10.1029/2001GB001466.

Lelieveld, J., P. J. Crutzen, and F. J. Dentener (1998), Changing concentration, lifetime and climate forcing of atmospheric methane, *Tellus, Ser. B*, *50*, 128–150.

Liss, P. S., and L. Merlivat (1986), Air-sea gas exchange rate: Introduction and synthesis, in *The Role of Air-Sea Exchange in Geochemical Cycling*, edited by P. Buat-Menard, pp. 113–127, Springer, New York.

Lowe, D. C., M. R. Manning, G. W. Brailsford, and A. M. Bromley (1997), The 1991–1992 atmospheric methane anomaly: Southern Hemisphere $^{13}C$ decrease and growth rate fluctuations, *Geophys. Res. Lett.*, *24*(8), 857–860, doi:10.1029/97GL00830.

Matsueda, H., H. Inoue, and M. Ishii (1993), Latitudinal distributions of methane in the upper troposphere and marine boundary air over the Pacific in 1990, *Geophys. Res. Lett.*, *20*(8), 695–698, doi:10.1029/93GL00510.

Mikaloff Fletcher, S. E., P. P. Tans, L. M. Bruhwiler, J. B. Miller, and M. Heimann (2004), CH4 sources estimated from atmospheric observations of $CH_4$ and its $^{13}C/^{12}C$ isotopic ratios: 1. Inverse modeling of source processes, *Global Biogeochem. Cycles*, *18*, GB4004, doi:10.1029/2004GB002223.

Millero, F. J., and A. Poisson (1981), International one-atmosphere equation of state of seawater, *Deep Sea Res., Part A*, *28*, 625–629, doi:10.1016/0198-0149(81)90122-9.

Monahan, E. C., and M. C. Spillane (1984), The role of oceanic whitecaps in air-sea gas exchange, in *Gas Transfer at Water Surfaces*, edited by W. Brutsaert and G. H. Jirka, pp. 495–503, Springer, New York.

Morimoto, S., S. Aoki, T. Nakazawa, and T. Yamanouchi (2006), Temporal variations of the carbon isotopic ratio of atmospheric methane observed at Ny Ålesund, Svalbard from 1996 to 2004, *Geophys. Res. Lett.*, *33*, L01807, doi:10.1029/2005GL024648.

Mosier, A., C. Kroeze, C. Nevison, O. Oenema, S. Seitzinger, and O. Vancleemput (1998), Closing the global $N_2O$ budget: Nitrous oxide emissions through the agricultural nitrogen cycle, *Nutr. Cycl. Agroecosyst.*, *52*(2/3), 225–248, doi:10.1023/A:1009740530221.

Naqvi, S. W. A., T. Yoshinari, D. A. Jayakumar, M. A. Altabet, P. V. Narvekar, A. H. Devol, J. A. Brandes, and L. A. Codispoti (1998), Budgetary and biogeochemical implications of $N_2O$ isotope signatures in the Arabian Sea, *Nature*, *394*, 462–464, doi:10.1038/28828.

Nevison, C. D., R. F. Weiss, and D. J. Erickson III (1995), Global oceanic emissions of nitrous oxide, *J. Geophys. Res.*, *100*(C8), 15,809–15,820, doi:10.1029/95JC00684.

Nevison, C., J. H. Butler, and J. W. Elkins (2003), Global distribution of $N_2O$ and the $\Delta N_2O$-AOU yield in the subsurface ocean, *Global Biogeochem. Cycles*, *17*(4), 1119, doi:10.1029/2003GB002068.

Nevison, C. D., T. J. Lueker, and R. F. Weiss (2004), Quantifying the nitrous oxide source from coastal upwelling, *Global Biogeochem. Cycles*, *18*, GB1018, doi:10.1029/2003GB002110.

Nightingale, P. D., G. Malin, C. S. Law, A. J. Watson, P. S. Liss, M. I. Liddicoat, J. Boutin, and R. C. Upstill-Goddard (2000), In situ evaluation of air-sea gas exchange parameterizations using novel conservative and volatile tracers, *Global Biogeochem. Cycles*, *14*(1), 373–387, doi:10.1029/1999GB900091.

Olivier, J. G. J., A. F. Bouwman, K. W. Van der Hoek, and J. J. M. Berdowski (1998), Global air emission inventories for anthropogenic sources of $NO_x$, $NH_3$ and $N_2O$ in 1990, *Environ. Pollut.*, *102*, 135–148, doi:10.1016/S0269-7491(98)80026-2.

Oudot, C., P. Jean-Baptiste, E. Fourre, C. Mormiche, M. Guevel, J.-F. Ternon, and P. Le Corre (2002), Transatlantic equatorial distribution of nitrous oxide and methane, *Deep Sea Res., Part I*, *49*, 1175–1193, doi:10.1016/S0967-0637(02)00019-5.

Owens, N. J. P., C. S. Law, R. F. C. Mantoura, P. H. Burkill, and C. A. Llewellyn (1991), Methane flux to the atmosphere from the Arabian Sea, *Nature*, *354*, 293–296, doi:10.1038/354293a0.

Ramaswamy, V., O. Boucher, J. Haigh, D. Hauglustaine, J. Haywood, G. Myhre, T. Nakajima, G. Y. Shi, and S. Solomon (2001), Radiative forcing of climate change, in *Climate Change 2001: The Scientific Basis.*

*Contribution of Working Group I to the Third Assessment Report of the Intergovernmental Panel on Climate Change*, edited by J. T. Houghton et al., pp. 349–416, Cambridge Univ. Press, Cambridge, U. K.

Rehder, G., and E. Suess (2001), Methane and $pCO_2$ in the Kuroshio and the South China Sea during maximum summer surface temperatures, *Mar. Chem.*, *75*(1–2), 89–108, doi:10.1016/S0304-4203(01)00026-3.

Rhee, T. S. (2000), The process of air-water gas exchange and its application, Ph.D. thesis, Tex. A&M Univ., College Station.

Robinson, C., et al. (2006), The Atlantic Meridional Transect (AMT) Programme: A contextual view 1995–2005, *Deep Sea Res., Part II*, *53*, 1485–1515, doi:10.1016/j.dsr2.2006.05.015.

Smith, S. R., M. A. Bourassa, and R. J. Sharp (1999), Establishing more truth in true winds, *J. Atmos. Oceanic Technol.*, *16*, 939–952, doi:10.1175/1520-0426(1999)016<0939:EMTITW>2.0.CO;2.

Suntharalingam, P., and J. L. Sarmiento (2000), Factors governing the oceanic nitrous oxide distribution: Simulations with an ocean general circulation model, *Global Biogeochem. Cycles*, *14*(1), 429–454, doi:10.1029/1999GB900032.

Swinnerton, J. W., and V. J. Linnenbom (1967), Gaseous hydrocarbons in sea water: Determination, *Science*, *156*, 1119–1120, doi:10.1126/science.156.3778.1119.

Trenberth, K. E., et al. (2007), Observations: Surface and atmospheric climate change, in *Climate Change 2007: The Physical Science Basis. Contribution of Working Group I to the Fourth Assessment Report of the Intergovernmental Panel on Climate Change*, edited by S. Solomon et al., pp. 235–336, Cambridge Univ. Press, Cambridge, U. K.

van der Werf, G. R., J. T. Randerson, G. J. Collatz, L. Giglio, P. S. Kasibhatla, A. F. Arellano, S. C. Olsen, and E. S. Kasischke (2004), Continental-scale partitioning of fire emissions during the 1997 to 2001 El Niño/La Niña period, *Science*, *303*, 73–76, doi:10.1126/science.1090753.

Walter, B. P., M. Heimann, and E. Matthews (2001), Modeling modern methane emissions from natural wetlands: 2. Interannual variations 1982–1993, *J. Geophys. Res.*, *106*(D24), 34,207–34,219, doi:10.1029/2001JD900164.

Walter, S., H. W. Bange, and D. W. R. Wallace (2004), Nitrous oxide in the surface layer of the tropical North Atlantic Ocean along a west to east transect, *Geophys. Res. Lett.*, *31*, L23S07, doi:10.1029/2004GL019937.

Wanninkhof, R. (1992), Relationship between wind speed and gas exchange over the ocean, *J. Geophys. Res.*, *97*(C5), 7373–7382, doi:10.1029/92JC00188.

Weiss, R. F. (1981), The temporal and spatial distribution of tropospheric nitrous oxide, *J. Geophys. Res.*, *86*(C8), 7185–7195, doi:10.1029/JC086iC08p07185.

Weiss, R. F., and B. A. Price (1980), Nitrous oxide solubility in water and seawater, *Mar. Chem.*, *8*(4), 347–359, doi:10.1016/0304-4203(80)90024-9.

Weiss, R. F., F. A. Van Woz, and P. K. Salameh (1992), Surface water and atmospheric carbon dioxide and nitrous oxide observations by shipboard automated gas chromatography: Results from expeditions between 1977 and 1990, *SIO 92–11*, 124 pp., Oak Ridge Nat. Lab., Oak Ridge, Tenn.

Wiesenburg, D. A., and N. L. Guinasso Jr. (1979), Equilibrium solubilities of methane, carbon monoxide, and hydrogen in water and sea water, *J. Chem. Eng. Data*, *24*(4), 356–360, doi:10.1021/je60083a006.

Woodruff, S. D., R. J. Slutz, R. L. Jenne, and P. M. Steurer (1987), A Comprehensive Ocean-Atmosphere Data Set, *Bull. Am. Meteorol. Soc.*, *68*(10), 1239–1250, doi:10.1175/1520-0477(1987)068<1239:ACOADS>2.0.CO;2.

Wuebbles, D. J., and K. Hayhoe (2002), Atmospheric methane and global change, *Earth Sci. Rev.*, *57*, 177–210, doi:10.1016/S0012-8252(01)00062-9.

Yoshida, N., H. Morimoto, M. Hirano, I. Koike, S. Matsuo, E. Wada, T. Saino, and A. Hattori (1989), Nitrification rates and $^{15}N$ abundances of $N_2O$ and $NO^{-3}$ in the western North Pacific, *Nature*, *342*, 895–897, doi:10.1038/342895a0.

Yoshida, O., H. Y. Inoue, S. Watanabe, S. Noriki, and M. Wakatsuchi (2004), Methane in the western part of the Sea of Okhotsk in 1998–2000, *J. Geophys. Res.*, *109*, C09S12, doi:10.1029/2003JC001910.

Zhang, G. L., J. Zhang, Y. B. Kang, and S. M. Liu (2004), Distributions and fluxes of methane in the East China Sea and the Yellow Sea in spring, *J. Geophys. Res.*, *109*, C07011, doi:10.1029/2004JC002268.

M. O. Andreae, Biogeochemistry Department, Max Planck Institute for Chemistry, P.O. Box 3060, D-55022 Mainz, Germany.

A. J. Kettle, Department of Earth Sciences, State University of New York at Oswego, Oswego, NY 13126, USA.

T. S. Rhee, Center of Polar Climate Sciences, Korea Polar Research Institute, Songdo Techno Park, Yeonsu-gu Songdo-dong 7-50, Incheon 406-840, Korea. (rhee@kopri.re.kr)